Hindawi
Indoor Air
Volume 2023, Article ID 9977685, 24 pages
https://doi.org/10.1155/2023/9977685

Research Article

A Monte Carlo Assessment of the Effect of Different Ventilation Strategies to Mitigate the COVID-19 Contagion Risk in Educational Buildings

Riccardo Albertin, Giovanni Pernigotto, and Andrea Gasparella

Faculty of Engineering, Free University of Bozen-Bolzano, Piazza Università 5, 39100 Bolzano, Italy

Correspondence should be addressed to Giovanni Pernigotto; giovanni.pernigotto@unibz.it

Received 13 January 2023; Revised 11 April 2023; Accepted 3 May 2023; Published 22 May 2023

Academic Editor: Xiaohu Yang

The COVID-19 pandemic outbreak has increased the general awareness of the importance of proper ventilation in the indoor environment to reduce the contagion risk. In particular, attention has been paid to specific categories of buildings, such as schools, due to two factors: (1) high occupancy density and (2) the presence of young and sometimes more susceptible people. Despite the high level of alertness towards the ventilation of classrooms, robust analyses of the effectiveness of the different strategies to mitigate the contagion risk have been difficult to perform. Indeed, the COVID-19 pandemic is still ongoing, and many factors, such as the presence of multiple viral strains, use of facial masks, progression in vaccination, and installation of air purifiers and other sanitization devices, make it difficult to fully quantify the impact of room ventilation by simply analysing available monitoring data. Moreover, mitigation strategies related to ventilation are often dynamic, increasing the complexity of the problem to assess. In this framework, this work proposes a new Monte Carlo method integrated with building performance simulation to evaluate the number of infected occupants under different scenarios, considering also the dynamic boundary conditions. The described approach has been applied to a case study classroom at the Free University of Bozen-Bolzano, Italy, analysing almost 100 different scenarios and discussing the effectiveness of different ventilation strategies traditionally adopted to ensure suitable IAQ according to CO_2 concentration limits. Results highlight the importance of combining different solutions (e.g., mixed-mode ventilation and facial masks) to limit the risk for both students and lecturers.

1. Introduction

Considering that the majority of people spend most of their life inside buildings, i.e., up to 90% of their time [1], concerns about indoor environmental quality are more than justified. Among other aspects, it is essential to assess indoor air quality IAQ inside homes, schools, offices, and public and private buildings to ensure the health of the occupants and plan interventions in case IAQ is not good enough [2].

Not only health but productivity as well can be affected by poor quality. In office environments, where the provision of a sufficient and continuous supply of fresh air to the occupants is often possible only by means of a ventilation system [3], office workers are exposed to different pollutants and environmental stressors, such as chemical, ergonomic, biological, and physical loads. These factors may affect work performance [4, 5], comfort [6], sickness leave rate [7–9], and the frequency of work-related health problems [10] and increase the possibility to develop sick building syndrome (SBS) symptoms [11–13].

The same aspects apply also to other building typologies. Focusing on schools, for instance, ASHRAE 62.1 [14] and 62.2 [15] provide a list of concentration limits for six pollutants (NO_2, CO, O_3, PM_{10}, SO_2, and lead) and impose a minimum flow rate of fresh air equal to $8\,l\,s^{-1}$ per person, to keep indoor CO_2 concentration below 700 ppm. This is also required to satisfy the odour perception quality of at least 80% of people. Most schools around the world have basic natural ventilation systems that are typically inadequate to meet the needs of students [16] leading to a nonnegligible risk for students to be exposed to various air pollutants. Kumar et al. [17] studied

the effects of poor air quality on students, highlighting again a potential risk of reduction in cognitive performances and of severe health consequences in the form of SBS.

Concentration levels of CO_2 are frequently used as a metric of IAQ [18] and are a critical aspect in classrooms for many different reasons, such as the students' health [19] and academic performances [20]. An increase of 10-20% in absenteeism in classrooms with an average CO_2 concentration above 1000 ppm was observed by Shendell et al. [21]. High levels of CO_2 concentration may be linked also to an increase in respiratory disease such as asthma [22] and a decrease in learning performances [13]. On the contrary, Bakó-Biró et al. [23] and Toftum et al. [24] observed that higher ventilation rates, and so, lower CO_2 concentrations, directly improve the responses for several tasks. For instance, according to Toftum et al. [24], learning outcomes for a group of Danish students exposed to lower CO_2 concentrations in schools got significantly better. Finally, Chatzidiakou et al. [25] presented an extensive review about IAQ in classrooms, highlighting that increased ventilation rates also help improve satisfaction with IAQ by mitigating overheating, reducing mould formation, and lowering total volatile organic compounds (TVOCs) and CO_2 concentrations.

Given the importance of keeping low CO_2 concentration levels in classrooms, different ventilation strategies aimed at improving IAQ have been widely analysed in the literature. Stabile et al. [26] and Almeida et al. [27] compared the effectiveness of different natural ventilation strategies in school buildings on indoor air quality. Stabile et al. [28] investigated the potential of both natural and mechanical ventilation strategies including free-running ventilation, based on the occupants' perception of IAQ.

Since the SARS-CoV-2 virus outbreak occurred in late 2019, it has become a priority to avoid conditions favourable to the virus spreading. For instance, Burgmann and Janoske [29] investigated the possibility to use air purifiers to reduce the airborne particles present in classrooms. In some cases, airborne transmission can be assumed as the main route of contagion [30], and so, the health hazard posed by the virus can be strictly correlated to IAQ as far as ventilation aspects are concerned. Consequently, ventilation strategies can be compared not only in terms of CO_2 concentration reduction but also in lowering the airborne contagion risk. A step in this direction has been made by Di Gilio et al. [31], who monitored the CO_2 levels in 11 classrooms of 9 schools and used CO_2 concentrations as a proxy to assess the airborne infection risk. A similar work has been proposed by Park et al. [32], who employed a tracer gas to measure the air flow rate related to different ventilation strategies and the Wells–Riley equation [33] for risk assessment.

Another useful model for risk assessment is the "airborne infection risk calculator" (AIRC) [34]. In this case, quanta concentrations, i.e., "the dose of airborne droplet nuclei required to cause infection in 63 % of susceptible persons," are directly used to assess the contagion risk. Despite the potential of this approach, it considers steady-state conditions and, thus, prevents the assessment of the effectiveness of dynamic strategies of ventilation and occupancy for the reduction of the contagion risk.

In this framework, this paper aims at investigating the efficacy of three standard and dynamic ventilation strategies, conventionally used for the CO_2 concentration reduction, namely, schedule-based, CO_2 concentration-based ventilation controls, and hybrid ventilation, to mitigate the SARS-CoV-2 infection risk. In order to do so, a new Monte Carlo approach has been proposed, ensuring the assessment of the contagion risk under dynamic boundary conditions and expanding in such a way the scope of state-of-the-art approaches, such as the AIRC by Buonanno et al. [30], which evaluates the contagion risk under steady-state conditions. The proposed methodology has been applied to a university classroom of the Free University of Bozen-Bolzano, focusing on the ability to mitigate the contagion risk of the ventilation strategies analysed in a previous contribution [35].

The proposed approach has overcome typical limitations related to transient boundary conditions, e.g., windows opening, variable number of infected subjects in the classroom, and CO_2 concentration-based control for mechanical ventilation. Furthermore, the Monte Carlo approach has also allowed considering the impact of some factors concurring in the infection process of healthy subjects, such as the probability of a subject being asymptomatic, a variable symptoms onset day for each subject, and the probability for an infected subject to be contagious before symptom onset, paving the way to a more comprehensive and dynamic infection risk assessment through all the COVID-19 contagion phases.

2. Methods

As previously stated, in this work, different ventilation strategies were evaluated in terms of COVID-19 contagion risk reduction. Furthermore, thanks to the steps required by the risk assessment process, it was possible to compare the ventilation strategies also in terms of CO_2 and energy load reduction. In fact, an energy simulation of the building model was necessary to calculate the air density of the classroom, a parameter that is included in the mass balance of the SARS-CoV-2 virus. Given the variety of factors included in the analysis, in the next paragraph, a brief overview of the steps involved in the evaluation processes is given.

The first phase was to select a case-study in order to create, calibrate, and validate a building model, necessary to dynamically calculate the temperatures in the classroom and so the energy required both for heating and cooling, under the adoption of different ventilation strategies. At this point, the software MATLAB® was used to implement a mass balance of both CO_2 and quanta of the SARS-CoV-2 virus, where a quantum is defined as "the dose of airborne droplet nuclei required to cause infection in 63 % of susceptible persons" [34]. To evaluate the risk of contagion due to COVID-19, both building model and mass balances were coupled with some of the AIRC tool's equations for the evaluation of the probability of contagion given the quanta concentration of COVID-19. Finally, a Monte Carlo approach was adopted to iteratively evaluate the risk of contagion by including some probabilistic factors such as the emission of quanta's rates by the infected occupants.

In this chapter, the aforementioned phases are described in detail.

2.1. Case Study. The case study selected for the model development is a classroom (named E5.21), located on the 5th and top floor of "E Building" at the Free University of Bozen-Bolzano campus, in the centre of the city of Bolzano (Northern Italy; 46° N, 11° E; altitude equal to 262 m). Conditions are typical of a heating-dominated climate in the Alpine region (2791 K d with respect to a base temperature of 20°C, calculated in agreement with DPR 412/1993 [36]), with a relatively short but hot summer. The "E Building" is surrounded by other buildings with approximately the same height.

The room floor area is 56 m^2, and its height is 3.5 m, with a total volume of 196 m^3. The classroom is surrounded by two other classrooms with similar features (E5.20 and E5.22), along a common hallway. It has two west-oriented windows and a single door of about 2 m^2 towards the corridor. Windows are located on one side of the classroom (single-sided natural ventilation), with a total surface of approximately 12 m^2. Each of the windows is divided into three portions—a fixed element, a tilt window, and a turn window. The openable area is about half of the total window area. Even if single-sided ventilation is generally related to lower ventilation rates with respect to cross-ventilation [32, 37], due to the configuration of the nearby buildings and no major obstacles in the proximity of the external wall, a good exchange of air is expected with the external environment when the windows are open.

Only two elements of the building envelope, i.e., the roof and the west façade, are exposed to the external environment: the former one is an insulated concrete slab covered by a green roof with a thermal transmittance equal to 0.21 W m^{-2} K^{-1}, while the latter one is an externally insulated concrete structure with a thermal transmittance equal to 0.24 W m^{-2} K^{-1}. The two windows are complex fenestration systems, i.e., triple glazing with integrated Venetian blinds with curved slats, with a thermal transmittance of 0.6 W m^{-2} K^{-1} and a solar heat gain coefficient (SHGC) of 0.53. Besides the integrated shading device, external Venetian blinds are present also.

The classroom is designed to host up to 24 students. In consideration of the typical activities (i.e., occupants seated, very light work), their metabolic rate can be assumed equal to 1.2 MET [38]. Five luminaires, each one with two fluorescent lamps, provide general illumination to the room, and two additional luminaires are dedicated to the blackboard. As a whole, the indoor artificial lighting system is responsible for 8.75 W m^{-2} of internal gains. Furthermore, a desktop computer, a beamer, and a motorized screen are installed in the room, contributing with other 1.7 W m^{-2}. Artificial lighting systems and equipment are typically on only during occupancy time, i.e., from Mondays to Fridays, from 8 : 00 am to 6 : 00 pm, and on Saturday in the morning, from 8 : 00 am to 12 : 00 pm.

The "E Building" is conditioned primarily by means of an air system, which supplies the indoor environments also with fresh air. During the heating period, which is from October 15th to April 15th in the climate zone where Bolzano is located, space heating needs are satisfied also by means of a couple of radiators per room, installed under the windows as a secondary heating system. All classrooms on the 5th floor are supplied by a ventilation system designed to provide a nominal air-flow rate slightly larger than 0.1 m^3 s^{-1} but generally operated at 0.07 m^3 s^{-1}.

Air conditioning, ventilation, and shadings are controlled through a central building energy management system (BEMS) by the University Facility Management, according to a typical schedule designed to ensure comfort conditions during occupancy time. Specifically, the systems are switched on at 6 : 00 am until 8 : 00 pm during weekdays and switched off during Sundays and holidays. On Mondays, the systems are switched on earlier, at 5 : 00 am, while on Saturdays they are turned off in the afternoon. In each room, the occupants are allowed to override the BEMS signals. For instance, although the nominal temperature setpoint is 22°C, the occupants can apply some regulation changes in a ±3°C range.

Classroom E5.21 is part of the Living Labs of the Free University of Bozen-Bolzano and is equipped with several sensors for the long-term monitoring of the indoor environmental conditions. Among the installed sensors, four onset HOBO U12-013 and two onset HOBO MX1102 loggers (Table 1) record air temperature and relative humidity with a 10-minute timestep and CO_2 concentrations with a 5-minute timestep, respectively. MX1102 sensors, in particular, are installed at approximately 1.75 m height (half of the room height), on the west façade between the two windows and on the opposite internal wall, sufficiently far away from the inlet and outlet vents of the air system to avoid their influence. The rooms adjacent to E5.21 and on the floor below are equipped with similar sets of sensors to allow for the monitoring of the same environmental quantities.

Finally, a meteorological station is installed on the roof of the "E Building," registering outdoor air temperature and humidity, and the solar radiation incident on different orientations (global and diffuse horizontal solar irradiance, global solar irradiance on the main cardinal vertical orientations, and direct normal irradiance).

In this research, two periods before the COVID-19 pandemic outbreak, characterized by similar occupancy profiles, were considered: period 1, from 18.11.2018 to 23.12.2018, and period 2, from 08.11.2019 to 23.12.2019. To be able to collect the data required for the calibration and validation processes, it was necessary to select two periods belonging before the start of the COVID-19 pandemic. In fact, during these periods, the number of students present in the classroom and typical occupancy were not yet affected by the pandemic.

2.2. Building Energy Simulation Model

2.2.1. Preparation, Calibration, and Validation. EnergyPlus 9.6 was employed to develop a single-zone building energy simulation (BES) model of the case study E5.21 classroom. Since the actual HVAC system serves the whole building, a simplified approach was adopted: specifically, an "ideal load air system" was modelled limiting air-flow rates and supply temperatures as in the real case-study, and additional heat gains were included to account for the radiators during the heating period.

The details provided in Section 2.1 were used as inputs. EnergyPlus contaminant mass balance model was exploited to simulate the variation of CO_2 concentration, setting the CO_2 generation rate per occupant in agreement with Persily and de Jonge [39]. In order to take into account the dilution

Table 1: Technical characteristics of the onset HOBO U12-013 and MX1102.

	Onset HOBO U12-013	Onset HOBO MX1102
Temperature sensor		
Range	-20 to 70°C	0 to 50°C
Accuracy	±0.35°C from 0 to 50°C	±0.21°C from 0 to 50°C
Resolution	0.03°C at 25°C	0.024°C at 25°C
Drift	<0.1°C per year	<0.1°C per year
Relative humidity RH sensor		
Range	5% to 95% RH (noncondensing)	1% to 90% RH (noncondensing)
Accuracy	±2.5% from 10% to 90% RH (typical), with a maximum of ±3.5%	±2% (20% to 80%: Typical to a maximum of ±4.5%, including hysteresis at 25°C; below 20% and above 80%: ±6% typical)
Resolution	0.05%	0.01%
Drift	<1% per year typical	<1% per year typical
Carbon dioxide sensor (sensing method: nondispersive infrared (NDIR) absorption)		
Range	—	0 to 5000 ppm
Accuracy	—	±50 ppm ±5% of reading at 25°C, less than 90% RH noncondensing and 1013 mbar
Resolution	—	Auto or manual to 400 ppm
Drift	—	<1% of FS

of CO_2 concentration because of airflows exchanged with the adjacent corridor, an equivalent generation rate was applied considering a dilution factor. Since it was observed that the E5.21 door was usually left open during the considered periods, a constant value was adopted.

Simulations were run considering a 5-minute timestep.

A multistage calibration was performed according to Penna et al. [40]. The first stage was dedicated to the calibration of surface heat convection coefficients and infiltration and ventilation rates, followed by a second stage focused on actual occupancy (i.e., number of people) and occupancy-dependent quantities, such as internal gains and CO_2 sources, as well as the CO_2 dilution factor because of air exchanges with the corridor (varied in a range between 0 and 1 according to a 0.1 step). Actual meteorological years (AMYs) were built for 2018 and 2019, thanks to the measurements collected by the weather station. Air temperatures recorded by the sensors in the adjacent environments were used as boundary conditions for internal walls and floor. After analysing, the recordings of CO_2 concentrations before room occupancy, 390 ppm and 420 ppm, were assigned as constant values of CO_2 concentration in the fresh air, respectively, for 2018 and for 2019. Finally, occupancy schedules were set in agreement with the data provided by the university secretariat. Simulated air temperature and CO_2 concentrations were compared to the values collected during period 1 (2018) and period 2 (2019), using the first period for calibration and the second one for validation purposes, expressing accuracy by means of the root-mean-square difference (RMSD) and the mean bias error (MBE). The RMSD values for air temperature in period 1 and period 2 resulted equal to 0.68°C and 0.70°C, respectively, and equal to 94 ppm and 76 ppm for the CO_2 concentration. The MBE values resulted equal to 0.54°C and 0.56°C for the air temperature and for periods 1 and 2, respectively, while the normalized MBE for CO_2 concentration was equal to 13% and 9.6%.

2.2.2. BES Simulation Plan. In order to explore the potential of different solutions for room ventilation and controls of the mechanical ventilation system, a simulation plan was designed.

Boundary and operative conditions were standardized. Instead of the AMY weather file, the reference year developed by the Italian Thermo-technical Committee (CTI) and the CO_2 outdoor concentration detected during the last months of 2019 (i.e., 420 ppm) was adopted.

Standard occupancy profiles were defined, with morning classes from 8 : 00 am to 12 : 00 pm and from 2 : 00 pm to 6 : 00 pm during weekdays. On Saturdays, only morning classes were scheduled, and no activities were simulated on Sundays. The standard calendar was implemented, assuming no occupancy during the winter holiday break (i.e., from 24.12 to 07.01) and in the month of August.

Conventional temperature setpoints of 20°C (space heating) and 26°C (space cooling) were set, starting 3 h before occupancy and for all the occupied time. Space heating was considered available only during the conventional heating season (from October 15th to April 15th) and space cooling when necessary. Air conditioning, ventilation, and shading controls were modelled adopting the same inputs, assuming the calibration results, with the exception of the maximum air flow rate for the ideal load air system, set equal to the value of 0.1 $m^3 s^{-1}$ indicated in Section 2.1.

The factors used to define different scenarios were selected based on their relationship with CO_2 concentrations in indoor spaces and, more in general, indoor air quality. Then, they were changed in order to reflect realistic situations, for example, a crowded classroom with no natural ventilation and a

closed door, or a low-density classroom with a CO_2-based mechanical ventilation. The factors selected are listed below:

(1) Number of occupants (i.e., 8, 16, or 24)

(2) Type of control for mechanical ventilation (i.e., scheduled occupancy-based or CO_2 concentration-based)

(3) Status of the classroom door, closed or open (i.e., CO_2 dilution factor equal to 1 or to 0.5)

With regard to factor (2), a CO_2-based mechanical ventilation system supplies additional fresh air within the limit of its nominal value (up to a total of 0.1 $m^3 s^{-1}$) to keep the CO_2 concentration level below a given threshold. Two different concentration setpoints were compared, i.e., 1220 ppm and 970 ppm, corresponding, respectively, to the lower thresholds for IAQ categories 2 and 1 according to EN 16798-1 : 2019 [41]. For those cases where mechanical ventilation was found insufficient, and in consideration of some of the policies adopted in educational buildings after the pandemic outbreak, also windows' opening was modelled, imposing 10 air changes per hour (ACH) according to three different schedules:

(a) From 9 : 45 am to 10 : 00, from 12 : 00 am to 2 : 00 pm, and from 3 : 45 pm to 4 : 00 pm

(b) Equivalent to (a), with the addition of 5-minute openings at the end of each hour

(c) Windows always open during all occupancy time

As regards to the dilution factor (factor 3), in the case of the open door, the same value found in the calibration and validation phases (i.e., 0.5) was adopted. Indeed, as mentioned before, the door was generally left open in the two periods considered for calibration and validation. For those scenarios that consider the door closed, a dilution factor of 1 was selected assuming the negligible contribution of infiltrations with the corridor.

Total simulated scenarios were 24 (Table 2). Among simulation outputs, operative temperatures and CO_2 concentrations during occupancy hours and annual space energy needs were analysed.

2.3. Modelling of the SARS-CoV-2 Infection Risk. Considering the SARS-CoV-2 infection risk, several previous contributions in the statistic field aimed at computing the probability of infection for subjects exposed to virus quanta.

The mathematical model on which the present work is based was developed by Riley et al. [33] based on data collected during and after an outbreak of measles in an elementary school in New York, in 1974. This model was later included as a particular case in the deterministic mathematical model by Gammaitoni and Nucci [42].

The mathematical model was used to simulate different environmental control strategies to reduce the infection risk in four scenarios of tuberculosis outbreaks. The quanta emission rate of airborne infection for an infected subject is a fundamental but difficult-to-know value to assess the probability of contagion. Because of that, data provided by the tuberculosis outbreaks were used to evaluate the probability of contagion without the need to calculate quanta emission rates for the infected occupants but by considering the final number of infected and noninfected people (a posteriori evaluation).

With the COVID-19 outbreak, a methodology to evaluate a priori the emission quanta rate was needed in order to quickly assess different strategies in terms of probability infection reduction, without waiting for enough data to be gathered for a posteriori evaluation. Buonanno et al. [34] estimated the quanta emission rate of SARS-CoV-2, obtaining as result distribution curves whose parameters depend on the activity performed by the infected subject. A mathematical model able to assess the risk of infection was then developed, based on the previous Riley model and the subsequent Gammaitoni and Nucci contribution. The final model for airborne contagion risk assessment has been implemented in the AIRC tool (airborne infection risk calculator) that can be used to evaluate the risk of contagion for different infectious diseases.

In the present work, some of the limitations of the AIRC tool related to transient boundary conditions (e.g., windows opening and variable number of infected subjects) are overcome by dynamically assessing the individual infection risk of subjects exposed to SARS-CoV-2 airborne transmission pathway with a Monte Carlo (MC) model. This methodology was used to evaluate the probability of infection for subjects exposed to SARS-CoV-2 in room E5.21 with the MC model written in MATLAB® environment. The ventilation strategies introduced in the previous chapter were analysed also in terms of effectiveness in airborne contagion risk reduction. The EnergyPlus model described in Section 2 was simplified and then integrated with a Monte Carlo model to dynamically evaluate not only the CO_2 concentrations but also the quanta concentration of COVID-19.

The following nomenclature was adopted in this research:

(i) *Infected/Noninfected*. A noninfected subject is a student or professor who never contracted the SARS-CoV-2 virus and can be infected only once per iteration, becoming an infected subject. Infected occupants can be either contagious or not, depending if the simulation day is inside their contagious period

(ii) *Contagious/Noncontagious*. A contagious subject is an infected subject during the contagious period. A noncontagious subject can be either a noninfected subject or an infected subject before or after the contagious period [43]

(iii) *Symptomatic/Asymptomatic*. All subjects are subdivided into one of these two categories at the beginning of each iteration, regardless of the infection status. The classification is needed only for the iteration-ending check process and does not contribute to changes during the simulations. Nonetheless, subjects classified as "asymptomatic" during the initialization phase, can be infected during the

Table 2: Characteristics of the simulated cases, including the number of occupants, the considered mechanical and natural ventilation strategies, and the door status.

Case ID	Number of occupants	Mechanical ventilation control	Natural ventilation	Status of the door
1A	8	Scheduled occupancy-based	No	Open
1B		IAQ category 2 CO_2-based		
1C		IAQ category 1 CO_2-based		
2A	16	Scheduled occupancy-based		
2B		IAQ category 2 CO_2-based		
2C		IAQ category 1 CO_2-based		
3A	24	Scheduled occupancy-based		
3B		IAQ category 2 CO_2-based		
3C		IAQ category 1 CO_2-based		
4A	8	Scheduled occupancy-based		
4B		IAQ category 2 CO_2-based		
4C		IAQ category 1 CO_2-based		
5A	16	Scheduled occupancy-based		
5B		IAQ category 2 CO_2-based		
5C		IAQ category 1 CO_2-based		
5D		IAQ category 1 CO_2-based	Schedule (a)	Closed
5E		IAQ category 1 CO_2-based	Schedule (b)	
5F		IAQ category 1 CO_2-based	Schedule (c)	
6A	24	Scheduled occupancy-based	No	
6B		IAQ category 2 CO_2-based		
6C		IAQ category 1 CO_2-based		
6D		IAQ category 1 CO_2-based	Schedule (a)	
6E		IAQ category 1 CO_2-based	Schedule (b)	
6F		IAQ category 1 CO_2-based	Schedule (c)	

simulations, furtherly increasing the spread of the SARS-CoV-2 virus

The implemented modelling approach is briefly described as follows:

(i) All iterations start with an infected asymptomatic subject (i.e., a student or a professor)

(ii) Due to the infected subject, when the simulations start, there is an increase in the total quanta emission in the classroom and, thus, of the quanta concentration in the next days

(iii) At the end of each day, it is checked if an infected symptomatic subject reaches the onset of symptoms or if all the asymptomatic infected ones end their contagious period, which would end the simulation as well. If neither of these two conditions is verified, another simulation day starts. The day on which the symptoms arise depends on the day of contagion and is selected randomly from a distribution curve for each infected subject

(iv) At the end of each day of the iteration, the number of infected subjects is quantified based on their exposure and risk, and the elapsed days from the start (day one) to the end of the iteration are evaluated

(v) Infected subjects are added to the quanta emission rates to assess the contagion risk on the following day

(vi) At the end of the simulation, the number of infected people is divided by the number of susceptible subjects to calculate the individual risk of contagion or "attack rate." This represents the percentage of people contracting the virus before one infected person is showing symptoms and the class is quarantined

2.3.1. Monte Carlo Model. The Monte Carlo model was used to run 1000 iterations for each scenario. During each iteration, several days are simulated (with a mean number that depends on the scenario selected) to dynamically evaluate the dose received by the susceptible subjects, and so, the possible number of infections, as well as accounting for some probabilistic features as the quanta emission rates, was selected randomly at each iteration from a distribution curve.

Before running the first simulation of each iteration, some variables and parameters are initialized:

(i) A random value of quanta emission rates and a set value of CO_2 emission rates are predetermined for

all subjects. While the values of quanta emission rate are different for all subjects and assigned only once at the start of each iteration, the value of CO_2 emission rate is equal for all subjects and kept constant for all scenarios (i.e., it is equal for all iterations and simulations)

(ii) The concentration of CO_2 in the classroom is set equal to the ambient concentration, while the concentration of quanta is set equal to zero

(iii) All subjects are randomly categorized either as symptomatic or as asymptomatic and as noninfected (except for subject 0 who is the infected asymptomatic person, either a student or a professor)

(iv) A weekly random schedule for each professor is created, ensuring 8 hours of lectures either in the morning and/or in the afternoon. Since 5 professors were considered to be involved, the 4 hours of Saturday morning are assigned randomly to one of the 5 professors (reaching a total of 12 lecture hours)

(v) Two different inhalation rate values are associated with the students and the professors, according to the activities that are, respectively, performed (such as standing and loudly speaking, activity usually related to professors, or sitting without speaking—related to the students)

After the initialization process, the simulation of the first day starts at 0 am. At the beginning of the lesson at 8 am, COVID-19 quanta are assumed to start being emitted according to the emission rate previously associated with subject 0.

During the simulations, all subjects emit CO_2 and one or more quanta of COVID-19, increasing both concentrations. At each timestep, the ventilation is evaluated based on the scenario's settings. At the end of each simulation, the total dose received from the subjects in the room is calculated as in equation (1) [30]:

$$D_q = \mathrm{IR} \sum_t n(t), \tag{1}$$

where IR is the inhalation rate and $n(t)$ is the quanta at each time step. The dose received by the subjects is equal for all the students but differs from the dose received by the professors, since the two categories of subjects have associated different inhalation rates ($0.49\,m^3\,h^{-1}$ for students and $0.54\,m^3\,h^{-1}$ for professors [44]. Furthermore, the dose received by each professor depends on the lecture's schedule: indeed, a professor may be present or not during the simulated day and only for a part of the day. The same approach applies also to the total quanta emitted in the classroom during occupancy hours, since a professor may contribute to increase quanta concentration only if infected and if present in the classroom.

Once the dose received by all subjects is evaluated, it is possible to assess the infection probability as in equation (2) [30]:

$$P_i(\%) = 1 - e^{-D_q}. \tag{2}$$

For each noninfected subject, a value between 0 and 100 is randomly extracted from a uniform distribution. If the given value is equal to or less than the infection probability, then a subject is considered to be infected. Then, four different factors are evaluated for the newly infected subjects: (a) quanta emission rate, (b) the symptom's onset day, and the (c) starting and (d) ending day of the contagious period.

At the end of each simulation, after the identification of the newly infected subjects, the algorithm checks if someone reaches the beginning or the ending of the contagious period. If so, the quanta emission rate for the given subjects is changed from 0 to the quanta emission rate evaluated during the initialization process, or vice versa.

Finally, the iteration ending conditions are checked: if (i) during a simulation, the onset day of an infected and symptomatic subject is reached or (ii) all the infected subjects are asymptomatic and not anymore contagious, the iteration stops. Indeed, it is assumed that, at the symptoms' onset, the subject is immediately tested for COVID-19, and so, the classroom is promptly quarantined. On the other hand, if all the infected subjects reached the end of the contagious period, no more infections are possible.

If the ending conditions are not met, some factors are initialized for the simulation of the next day: it is checked if the next day is either a weekday (or Saturday morning) or Sunday. In case the next day is Sunday, all the internal conditions of the classroom are reset: CO_2 concentration is set equal to the external ambient one and COVID-19 concentration to zero thanks to the infiltration rate. Otherwise, if the next day is a weekday, the concentrations of the last time step of the previous day (i.e., 23 : 59) are used as the initial value for the day after. It is worth mentioning that both viral inactivation and particle deposition rates are considered in the analysis, with values of $0.63\,h^{-1}$ and $0.24\,h^{-1}$, respectively [44].

After the initialization of the variable for the next day, a new simulation starts, and the whole process is repeated until one of the two ending conditions is met. At the end of each iteration, the total number of infected (symptomatic or asymptomatic) is counted, as well as the number of days needed to reach the ending condition.

A scheme of the proposed Monte Carlo model is reported in Figure 1.

In the next paragraphs, more details are provided regarding the four factors previously mentioned, evaluated for the newly infected subjects: (a) quanta emission rate, (b) symptoms' onset day, and (c) starting and (d) ending day of the contagious period. In addition, the (e) asymptomatic selection process is investigated and the (f) simplified building model is described.

Quanta emission rates (a) depend on the subject's activity. Two possible activities are selected for the students: resting–breathing, to consider the time spent by the students listening to the lecture, and resting–speaking, to consider those moments where the students speak to each other or to the professor (Table 3). Two activities are selected also for the professors:

resting–speaking and standing loudly–speaking. It is supposed that the professor spends most of the time standing while lecturing the students, with some moments when the professor speaks to the students while sitting. It was then possible to classify the activities as a primary activity (the one that is performed for most of the time) and a secondary activity, for both students and professors. A weight between 0 and 1 is assigned to the secondary activity, randomly choosing each subject from a normal distribution having a mean equal to zero and three standard deviations equal to the maximum fraction of time that is possible to allocate to the secondary activity. The primary activity is assumed to be performed for a fraction of time which is complementary to the weight of the secondary one.

This allows us to estimate an individual average quanta emission rate from the individual activity-related rates. Quanta emission rates for each activity are assigned with a lognormal distribution, the parameters of which, i.e., mean and standard deviation of logarithmic values, depending on the subject's activity [30].

For the infected subjects, the individual quanta rate emitted during the contagious period is selected randomly by setting a maximum percentage of time that can be dedicated to the secondary activity to 30%. The quanta emission rates are assumed constant for all the occupancy hours inside the contagious period.

Symptoms' onset day (b) and start (c) and end (d) of the contagious period are strictly related. Firstly, when a subject is infected, the onset day is selected according to a gamma distribution whose parameters are a shape equal to 5.81 and a rate of 1.06 [45]. Given the onset day, it is then possible to evaluate the starting day of the contagious period according to a gamma distribution whose parameters are a shape of 97.188, a rate of 3.719, and a shift of 25.625 [46]. In this case, the starting day is evaluated with respect to the onset day. This means that the starting day of the contagious period (i.e., the number of days before the onset day) is always a negative or null value, and so, an infected subject can be contagious even before the symptoms' onset day. This is representative of the reality: in their study, He et al. [46] highlighted how infected people can be contagious even 2-3 days before the symptom onset. The contagious period may start before the symptoms' onset day for both symptomatic and asymptomatic subjects. Under no circumstances, the starting day may be set before than two days apart from the infection day. The ending day, on the other hand, is not evaluated randomly but set equal to the 9^{th} day after the symptoms' onset day for all subjects, in order to consider the worst-case scenario. In fact, after 8 days from symptom onset, the live virus can no longer be cultured from infected subjects, indicating a significant infectiousness decline [46].

The probability of being asymptomatic (e) is evaluated by means of a Gaussian distribution with a mean of 40.5 and a standard deviation of 3.5 for each subject. Then, as for the infection probability, a number in the range of 0-100 is extracted for all subjects with a uniform distribution. A subject is considered to be asymptomatic if the extracted number is less than the probability value. The Gaussian distribution parameters have been developed accordingly to the data provided by Ma et al. [47].

2.3.2. Scenarios. All 24 scenarios introduced in Section 2.2.2 were run with the Monte Carlo model coupled with the simplified building model. Some hypotheses, equal for all scenarios, were made prior to the start of the iterations. As a first hypothesis, all the students do not change classrooms during the day or during the week. The students stay in the classroom from 8 am to 12 pm (all weekdays including Saturday) and from 2 pm to 6 pm (from Monday to Friday). During the occupancy hours, a professor is always present, and he/she may change from morning to afternoon and from day to day, with a random schedule created before running the simulations and thus equal for all of them. It has been hypothesized that 5 professors teach in the classroom, for a total of 8 hours each plus the 4 hours on Saturdays that are assigned randomly to one of the professors.

It was also necessary to consider the typology of the starting infected subject (student or professor), since it affects the quanta emission rate and the occupancy hours of the infected subjects in the classroom, increasing the number of scenarios to 48. Furthermore, all scenarios were evaluated again (1) with the hypothesis that both students and professor are wearing masks and (2) by considering the simultaneous occurrence of two subjects 0 (in this case, both students) without mask utilization, representative of a more advanced stage of progression of the pandemic. The final number of scenarios is 96, for a total of 96000 iterations and circa 1344000 building simulations. It is worth underlining that in this research, the overall risk of contagion for the occupants in the classroom was assessed, without a specific distinction between the contagion risk for professors and for students.

2.3.3. Postprocessing of the Results. As mentioned before, the attack rate of the classroom was calculated at the end of each iteration. However, in order to properly compare the results, it was necessary to cluster them by means of the number of students, since the attack rate is relative to the total number of susceptible subjects.

For simplicity, as for the list of scenarios, the results are reported with the same designations for both typologies of subject 0 with an additional letter "*p*" or "*s*", which stands for "professor" and "student," respectively.

Furthermore, the graphs reporting CO_2 and quanta concentrations for different scenarios were obtained by considering only one infected subject (i.e., subject 0) in the classroom, without the possibility for other subjects to be infected at day 0. Quanta emission rate for the infected subject represented in the charts was set equal to the mean value of the distribution curve related to his main activity, while CO_2 emission rates were not changed.

3. Results and Discussion

3.1. CO_2 Concentration and Operative Temperature. Figures 2 and 3 report CO_2 concentrations and operative temperatures for each scenario. In each box, the horizontal line represents the median value, while the upper and lower part of the boxes represent, respectively, the 5^{th} and 95^{th} percentiles of the data. Simulated data refer only to the occupancy time during the whole year.

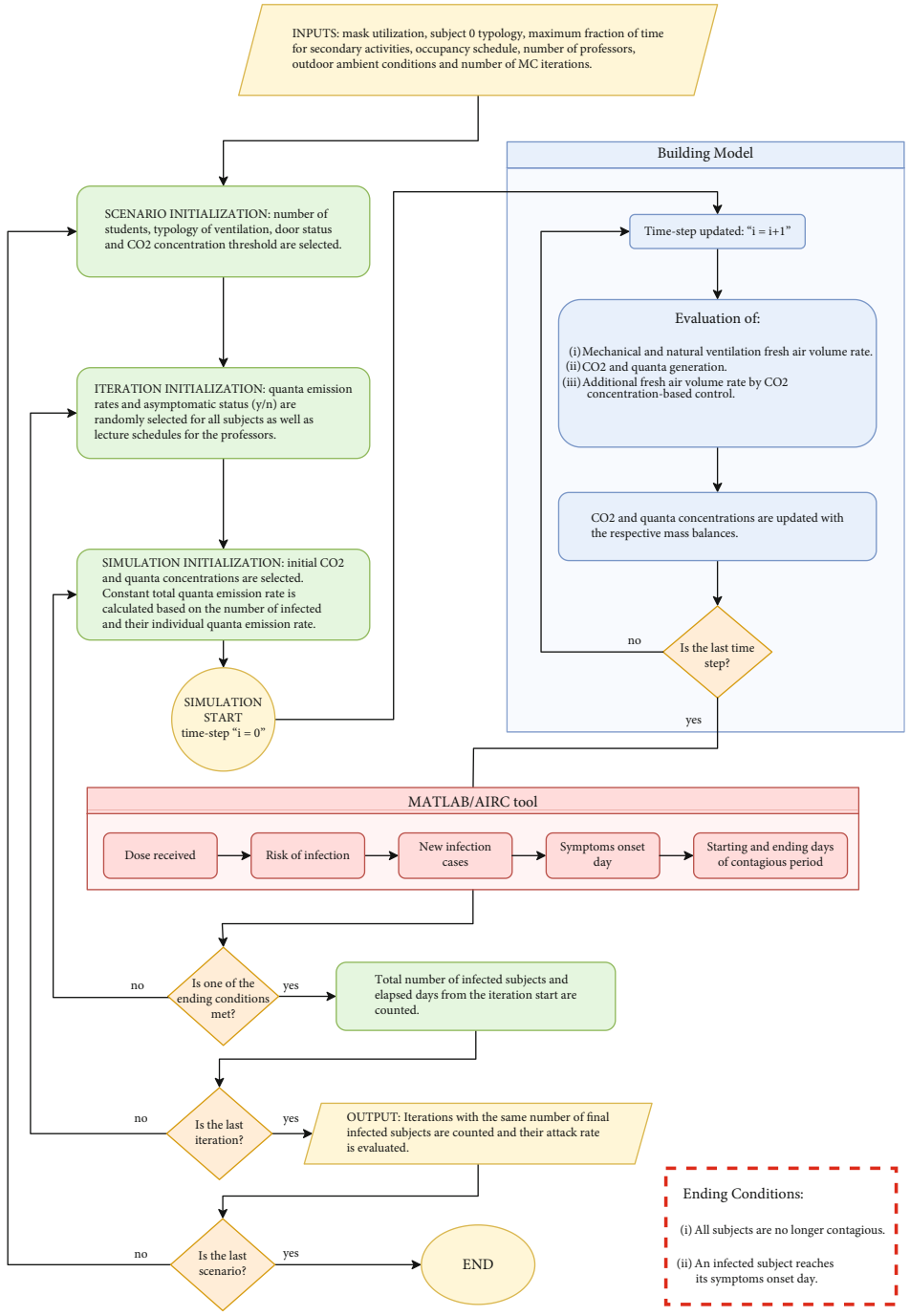

Figure 1: Scheme representation of the proposed Monte Carlo model.

Table 3: Lognormal distribution curve's parameters for different activities.

Activity	Log mean	Log std.	Subjects	Type
Resting–breathing	-0.43	0.73	Students	Primary
Resting–speaking	0.24	0.72	Student and professors	Secondary
Standing loudly–speaking	1.08	0.72	Professors	Primary

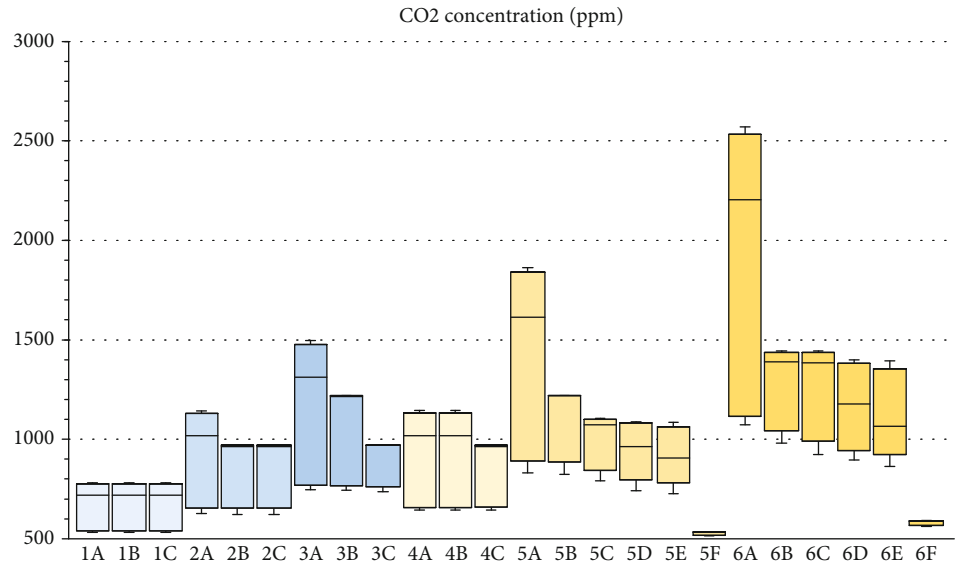

Figure 2: Boxplots representing the CO_2 concentrations during occupancy time. The boxes indicate the 5^{th}-95^{th} percentile range, and the horizontal line is the median. Light blue, blue, and dark blue represent, respectively, the group of cases with 8, 16, and 24 students with the open door. On the contrary, light yellow, yellow, and dark yellow indicate the same groups with the closed door.

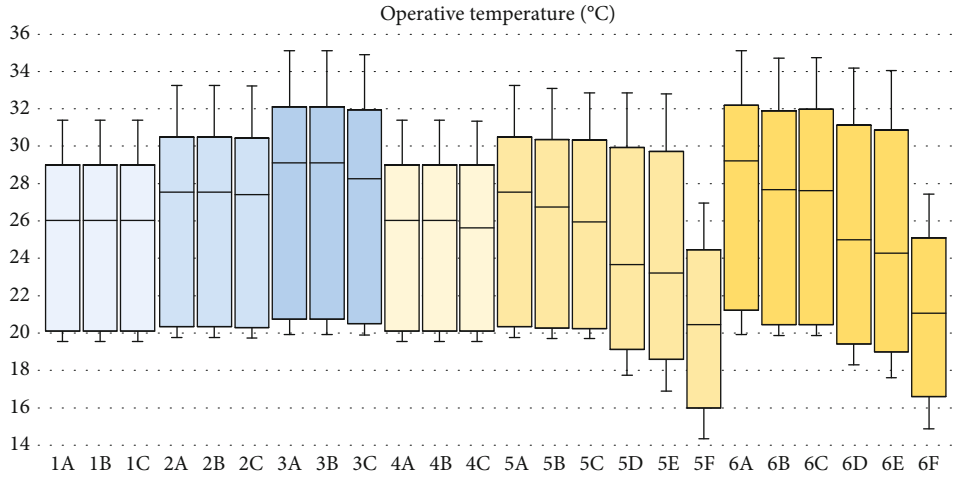

Figure 3: Boxplots representing the operative temperatures during occupancy time. The boxes indicate the 5^{th}-95^{th} percentile range, and the horizontal line is the median. Light blue, blue, and dark blue represent, respectively, the group of cases with 8, 16, and 24 students with the open door. On the contrary, light yellow, yellow, and dark yellow indicate the same groups with the closed door.

As observed in the charts, CO_2-based controls (indicated with the letters B and C) have little effect on the CO_2 concentrations in the classroom when the door is left open and the occupancy density is low or average (i.e., 8–16 students). Case 2C is an exception, and if the CO_2-based controls are set to keep the IAQ category 1, the 95^{th} percentile value of CO_2 concentration lowers significantly. On the contrary, CO_2-based controls are necessary if the occupancy density is high (i.e., 24 students), even when the door is open, to lower the CO_2 concentrations below either IAQ categories 1 and 2 thresholds (see cases 3B and 3C).

In the case of closed door and low occupancy density, CO_2-based controls are needed only to achieve IAQ category 1 target (case 4C, represented in Figure 4), and natural ventilation is enough to guarantee category 2. However, with medium or high occupancy density, the mechanical ventilation system struggles to provide enough fresh air to lower the CO_2 concentration below the prescribed thresholds (see cases 5B, 5C, 6B, and 6C represented in Figures 5 and 6). For this reason, it is necessary to adopt a mixed ventilation strategy by coupling mechanical ventilation with natural ventilation. Nevertheless, even with the additional supply provided by the occasional opening of the windows, it is possible to achieve only IAQ category 2 targets in the case of medium occupancy density (see cases 5D and 5E). In the case of full occupancy and closed door, the only way to satisfy the IAQ targets is to leave the windows open during the whole period of occupancy. As a result, it is possible to reduce the median

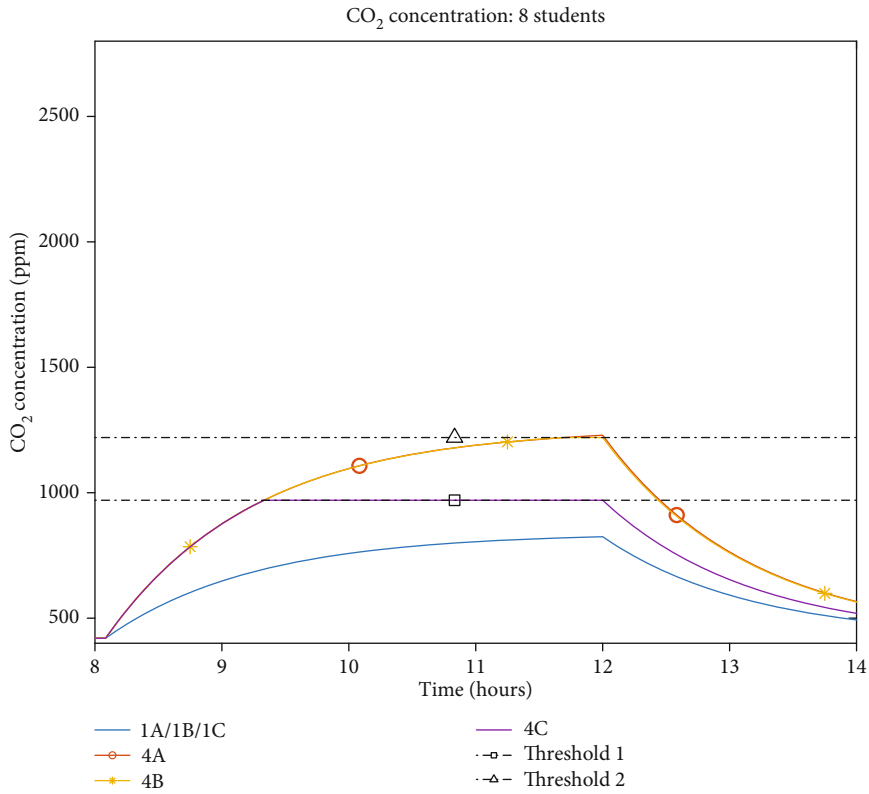

Figure 4: CO_2 concentration profiles for those scenarios with 8 students that consider the door open (1A, 1B, and 1C) or closed (4A, 4B, and 4C), schedule-based (1A and 4A), or CO_2-based mechanical ventilation, either with a threshold of 1220 ppm (1B and 4B) or 970 ppm (1C and 4C).

value of CO_2 concentration to a slightly larger value with respect to the outdoor one.

Regarding the indoor operative temperature, as expected, it increases with a trend that is proportional to the number of occupants and inversely proportional to the rate of fresh air supply. The operative temperature can reach values larger than 30°C during the summer months and in the earliest occupancy hours, if the room is at full capacity, and values as low as 15°C in the winter months if the windows are left open for all the occupancy period. Cold and hot temperatures are due to the capacity of the simulated system, which has the same features as the actual one.

The number of occupants affects also the heating and cooling needs. Considering the standard occupancy-based controls for mechanical ventilation (indicated by the letter A), it can be noticed that the heating energy required by the classroom ranges from a minimum of 254 kWh (cases 3A and 6A with 24 students) to a maximum of 690 kWh (cases 1A and 4A with 8 students) and from 1696 kWh (1A and 4A) to 2484 kWh (cases 3A and 6A) for the cooling (Figure 7). CO_2-based controls can have a significant effect on the energy needs: in fact, we can observe an increase in the energy for space heating with respect to the cases with occupancy-based controls, respectively, by +99% for case 3C, +65% for 5B, +104% for 5C, +133% for 6B, and+145% for 6C. For the same cases, the energy required for cooling lowers by a range from 15% to 25%, depending on the specific configuration (Figure 8). Windows opening further increases the energy required for heating (5D: +289%; 5E: +324%; 5F: +309%; 6D: +471%; 6E: +552%; and 6F: +542%) while decreasing the cooling needs with a lower magnitude (5D: -28%; 5E: -34%; 5F: -94%; 6D: -34%; 6E: -36%; and 6F: -93%). It is also interesting to notice that the constant opening of windows during the whole occupancy time has no significant impact on the heating needs, with an increase for cases 5F and 6F even lower than cases 5E and 6E; on the contrary, it can have a remarkable effect on the cooling needs, reduced by more than 90%, i.e., almost three times more compared to the other cases.

3.2. Modelling of the SARS-CoV-2 Infection Risk. This section has been furtherly subdivided into chapters, grouping the results under 6 categories in order to better understand the impact of (1) subject-0 typology, (2) door status (open or closed), (3) ventilation strategies, (4) mask adoption, and (5) number of initial infected. Attack rate results are reported in Figures 9–11.

3.2.1. Subject-0 Type. The first aspect taken into consideration is if the presence of a different initial infected subject, either a professor or a student, has a significant impact on the results. Figures 9–11 compare the attack rate in the case the initial infected subject is either a student (label "s" in the charts, on the left) or a professor (label "p" in the chart, on the right). It is possible to notice that the difference in terms of attack rate is generally small or negligible. This could be explained by the fact that, although higher quanta emission

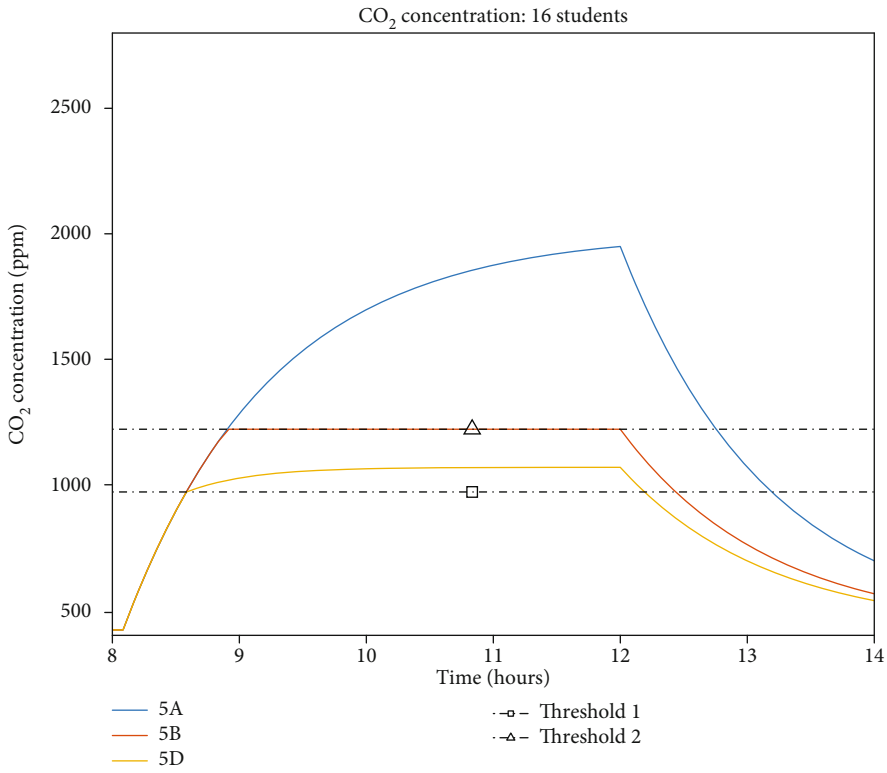

Figure 5: CO_2 concentration profiles for those scenarios with 16 students, closed door, without natural ventilation, and schedule-based (5A) or CO_2-based mechanical ventilation, either with a threshold of 1220 ppm (5B) or 970 ppm (5C).

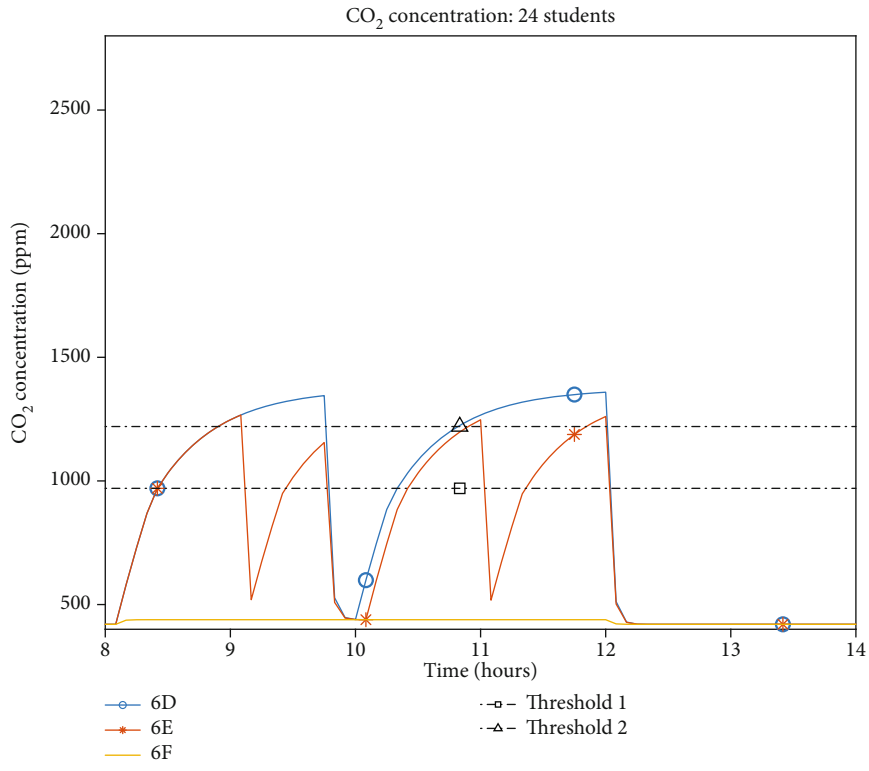

Figure 6: CO_2 concentration profiles for those scenarios with 24 students, closed door, and with natural ventilation either with schedule "a" (6D), "b" (6E), or "c" (6F).

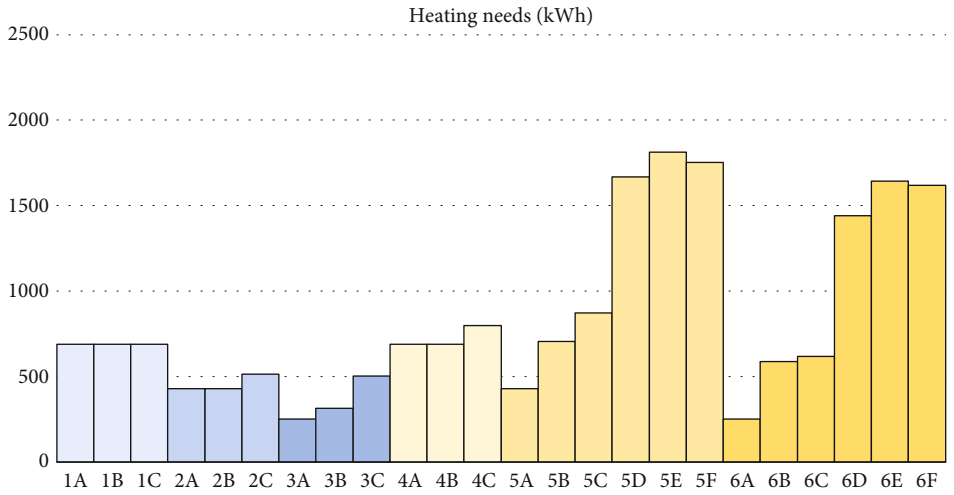

Figure 7: Energy needs for space heating in each scenario. Light blue, blue, and dark blue represent, respectively, the group of cases with 8, 16, and 24 students with open door. On the contrary, light yellow, yellow, and dark yellow indicate the same groups with a closed door.

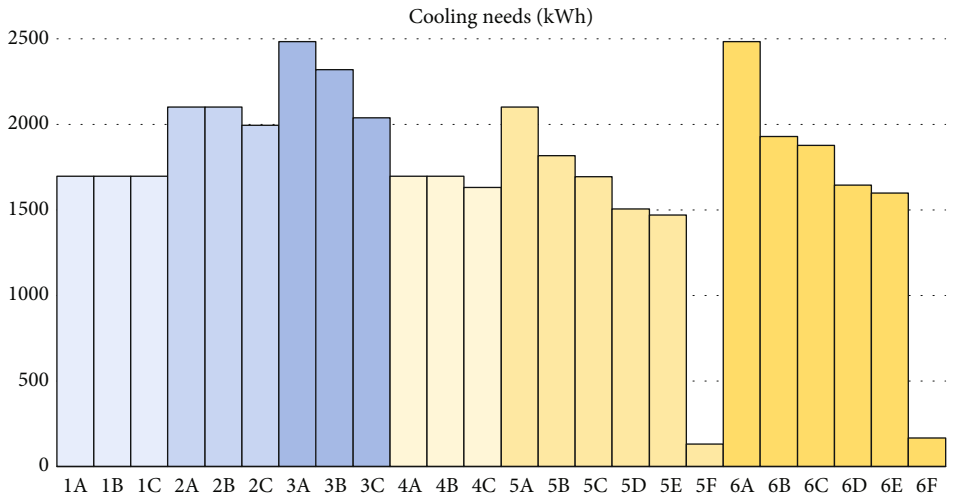

Figure 8: Energy needs for space cooling in each scenario. Light blue, blue, and dark blue represent, respectively, the group of cases with 8, 16, and 24 students with open door. On the contrary, light yellow, yellow, and dark yellow indicate the same groups with a closed door.

rates characterize the professors' activities, this is balanced by the fewer hours of presence in the classroom. The major difference lies only in the cluster with 24 students (comparing, for instance, 3As with 3Ap and 6Ds with 6Dp), with a slightly larger attack rate if the initial infected subject is a student. Despite these differences, cases 5A and 6A were identified as the worst cases, both for students and professors.

It can be concluded that, considering the overall contagion risk in the case study environment, it could be generally safer to limit exposure time between susceptible subjects rather than to act on the activities performed to lower the quanta emission rate of the infected subjects.

The elapsed days from the start of each iteration are reported for those scenarios with one infected student as subject-0, without mask utilization (Figures 12–14). The count neglects all those cases where subject-0 did not infect any other subject. It is possible to observe that in all scenarios, regardless of the number of students, door status, or ventilation strategy, the median of elapsed days is always equal to 10. This is related to the evaluation process of the ending day of the contagious period: in order to consider the worst-case scenario, the elapsed time from the symptoms' onset day to the last day of the contagious period was set equal to 9 for all the infected subjects. Nonnegligible is the count of iterations that ended during the contagious period of subject-0. This aspect is partially related to the probability for an infected subject to be contagious also before the symptoms' onset day, highlighting the necessity of high ventilation rates as a prevention strategy.

3.2.2. Door Status. The second analysed aspect was the impact of the state of the door, open or closed. As shown in Figure 11, it can be observed that it has a significant impact on the attack rate for both median and maximum values when the occupancy density of the classroom is high

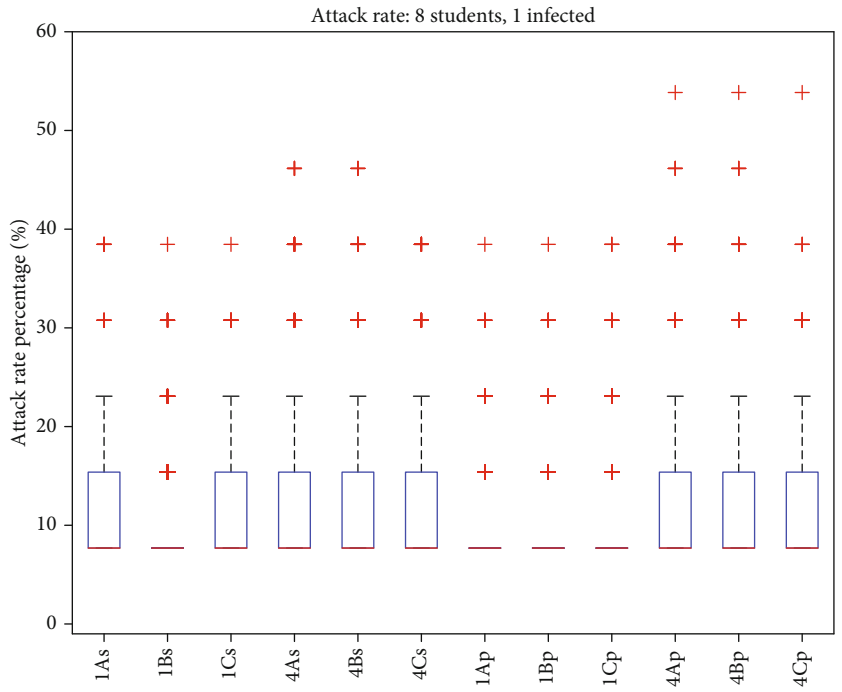

Figure 9: Boxplots indicating the 25th-75th percentile range representing the attack rate for those scenarios with 8 students. "s" and "p" indicate student or professor as the initial infected subject.

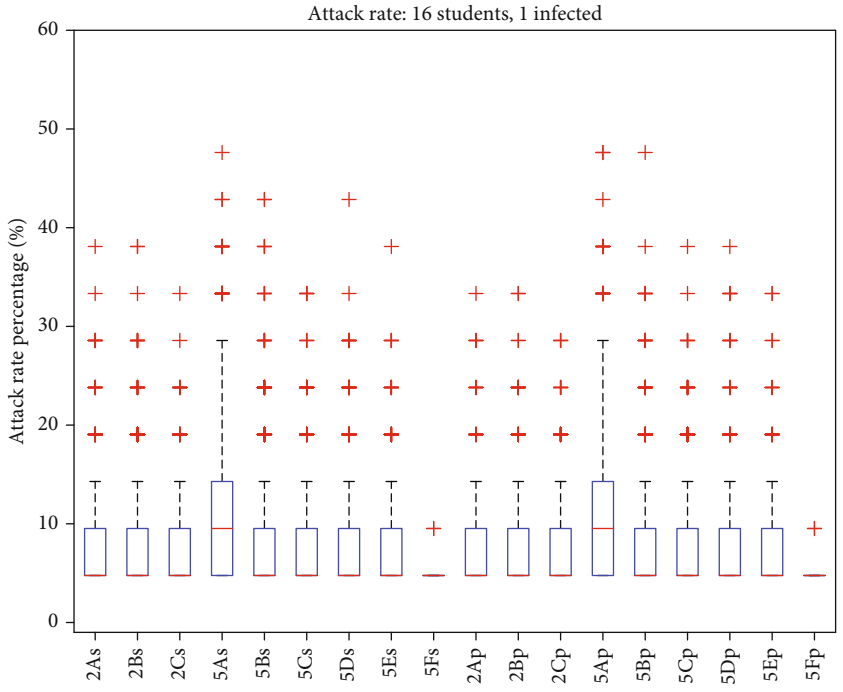

Figure 10: Boxplots indicating the 25th-75th percentile range representing the attack rate for those scenarios with 16 students. "s" and "p" indicate student or professor as the initial infected subject.

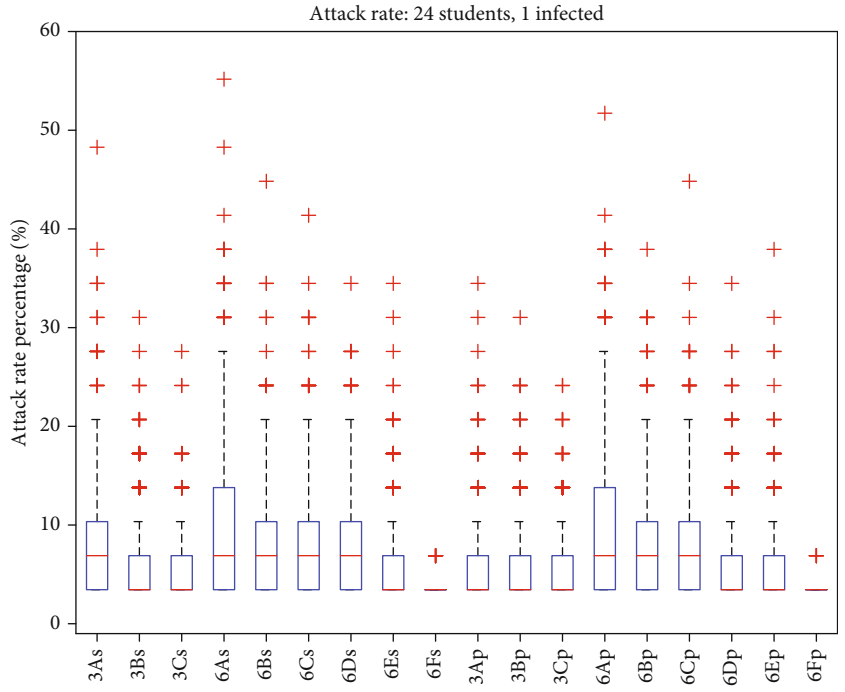

Figure 11: Boxplots indicating the 25th-75th percentile range representing the attack rate for those scenarios with 24 students. "s" and "p" indicate student or professor as the initial infected subject.

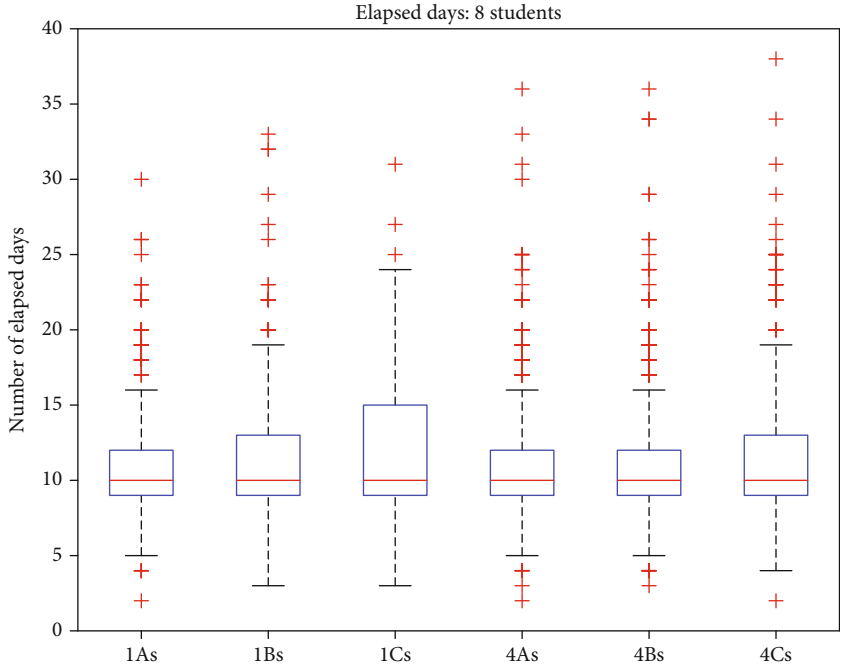

Figure 12: Boxplots indicating the 25th-75th percentile range representing the number of elapsed days for those scenarios with 8 students.

(24 students, scenarios 3Cs and 6Cs): when the door is open, indeed, the attack rate is the lowest.

It can be concluded that, since keeping the door open is an easily employable strategy to reduce the concentration of contaminants in the room, it should be adopted regardless of the number of occupants.

3.2.3. Ventilation Strategies. Focusing on the different ventilation strategies, a strict correlation with the occupancy density and with the status of the door is noticed.

Looking at the results of the cases with a student as subject-0, if the number of students is 8 (Figure 9), it seems unnecessary to adopt advanced CO_2 concentration-based

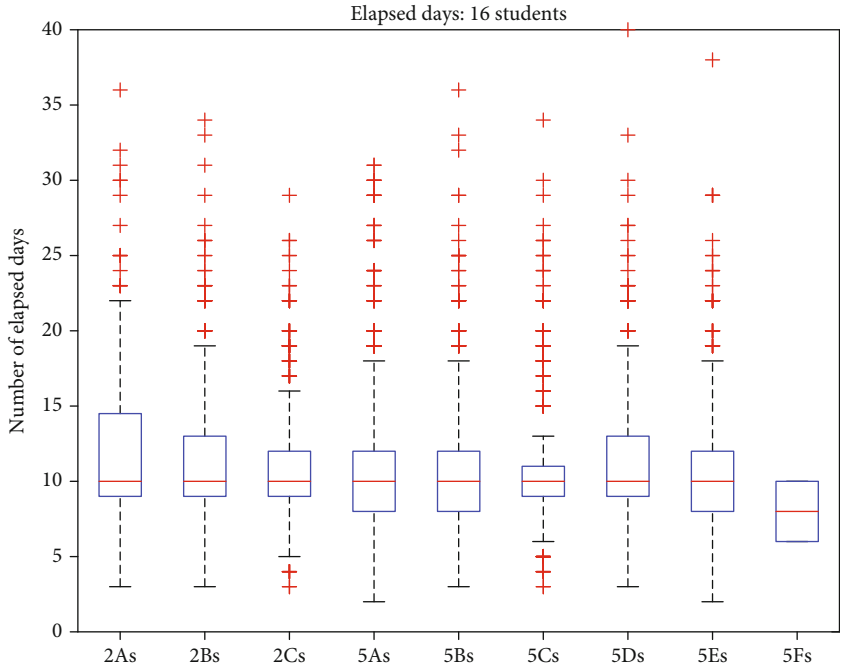

Figure 13: Boxplots indicating the 25th-75th percentile range representing the number of elapsed days for those scenarios with 16 students.

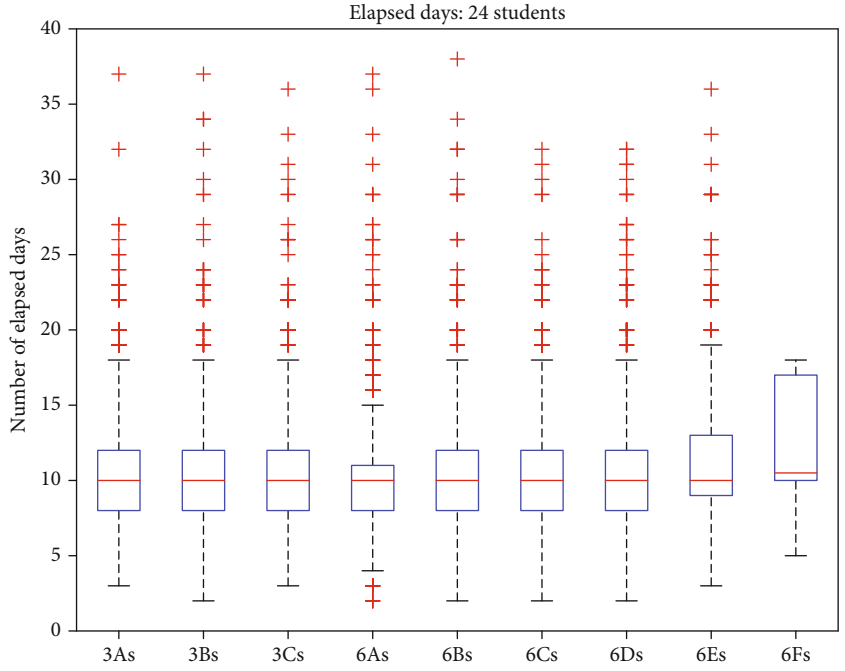

Figure 14: Boxplots indicating the 25th-75th percentile range representing the number of elapsed days for those scenarios with 24 students.

controls since they have no effects on the attack rate. This can be explained, for instance, considering the simulated profiles of CO_2 concentration discussed in Section 3.1: both CO_2 thresholds (either 1220 ppm or 970 ppm) are never reached, and so, no additional fresh air is supplied compared to the standard scheduled control of the mechanical ventilation. The difference in the results for case 1Bs compared to cases 1As and 1Cs is to be attributed to the probabilistic approach used for the evaluation of the number of infected subjects.

This is not the case for the cluster with 16 students (Figure 10): for instance, considering the cases 5As and 5Ap with the door closed, it can be noticed that the scheduled control of the mechanical ventilation is not adequate,

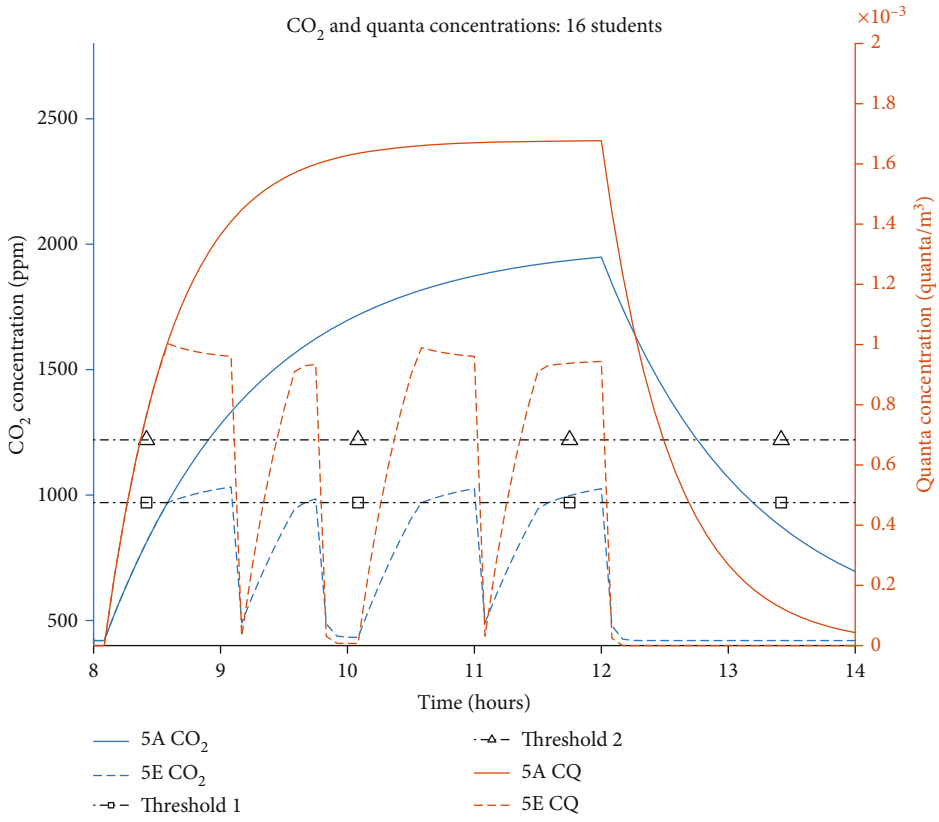

Figure 15: CO_2 and COVID-19 quanta concentration profiles for scenarios 5A and 5E.

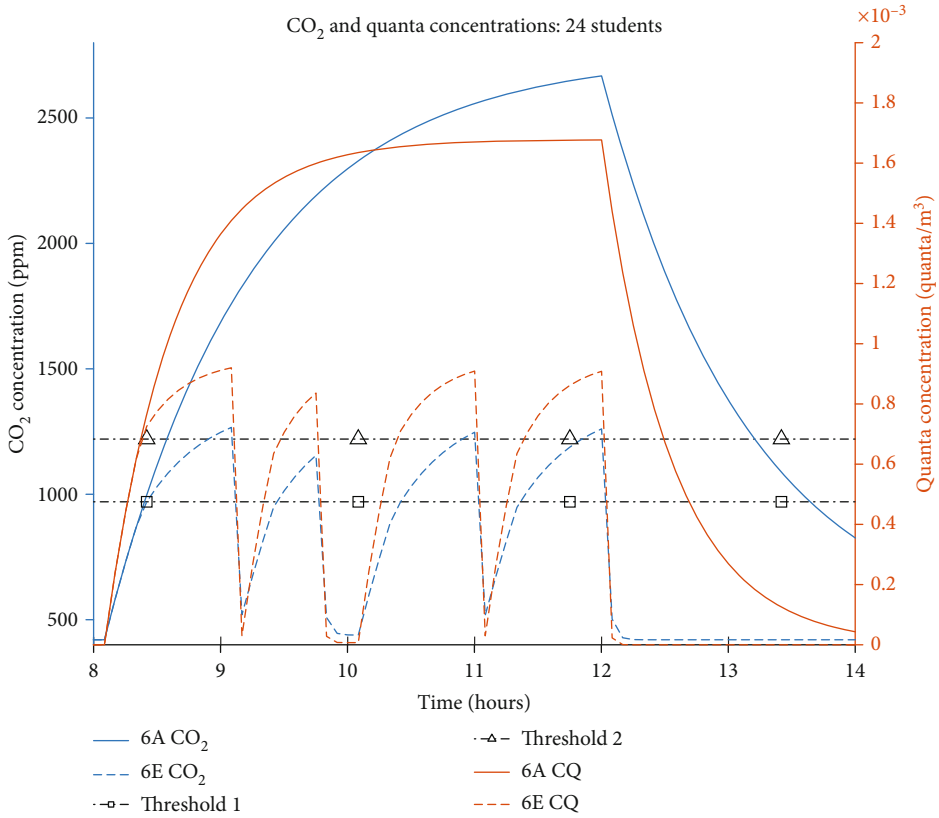

Figure 16: CO_2 and COVID-19 quanta concentration profiles for scenarios 5A and 5E.

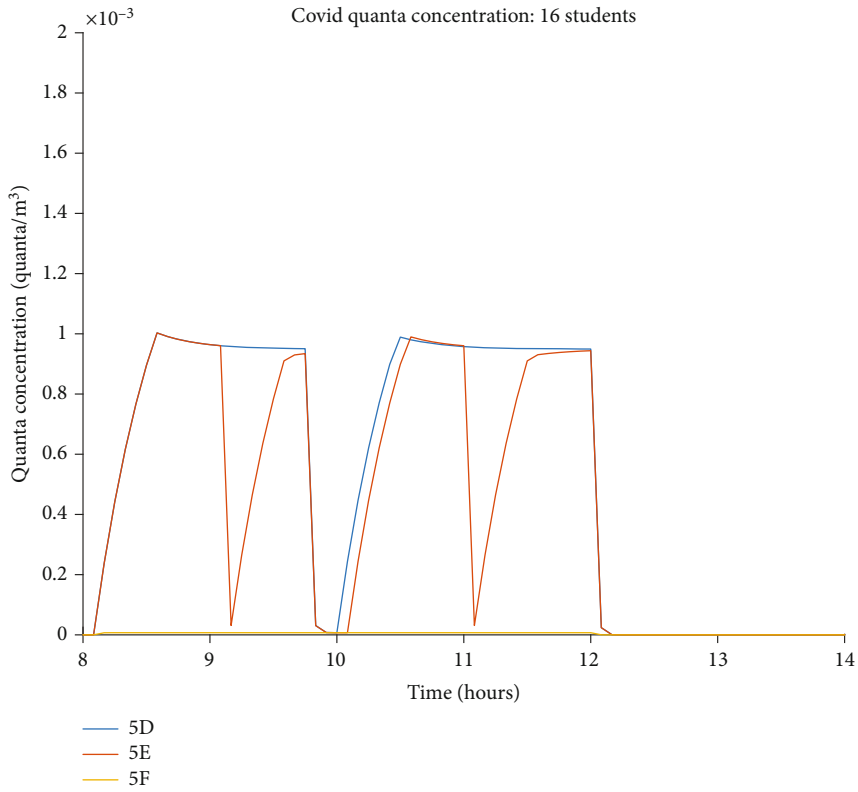

Figure 17: COVID-19 quanta concentration profiles for scenarios 5A, 5E, and 5F.

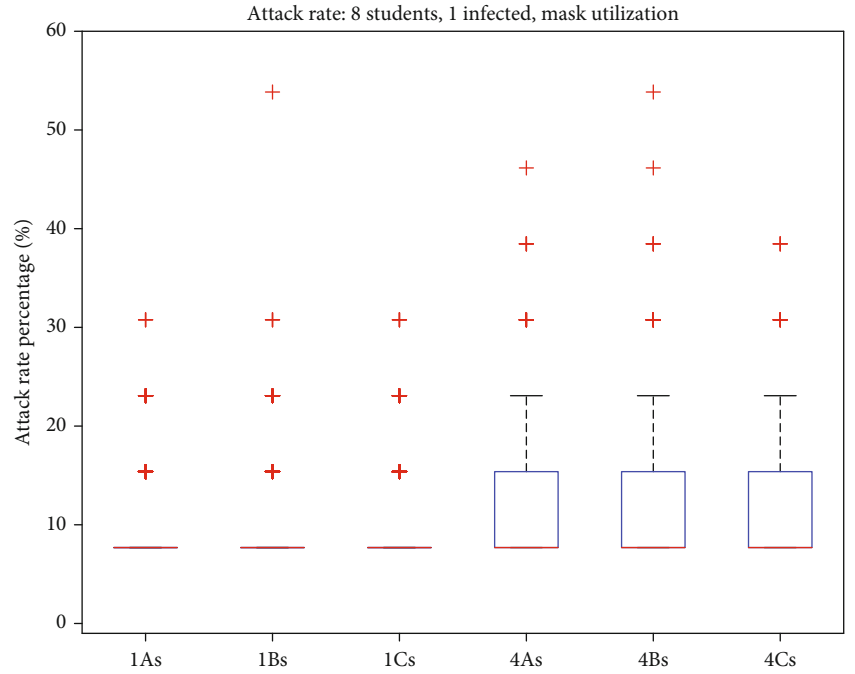

Figure 18: Boxplots indicating the 25^{th}-75^{th} percentile range representing the attack rate for those scenarios with 8 students and mask utilization and subject-0 being a student. As a comparison, the results of the same scenarios without mask utilization can be found in Figure 9, Section 3.2.

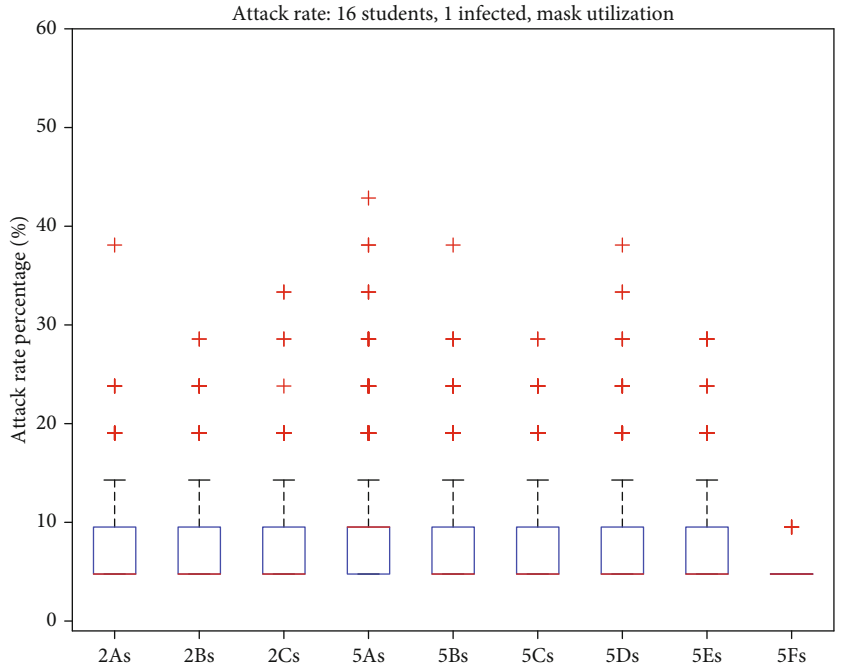

FIGURE 19: Boxplots indicating the 25th-75th percentile range representing the attack rate for those scenarios with 16 students and mask utilization and subject-0 being a student. As a comparison, the results of the same scenarios without mask utilization can be found in Figure 10, Section 3.2.

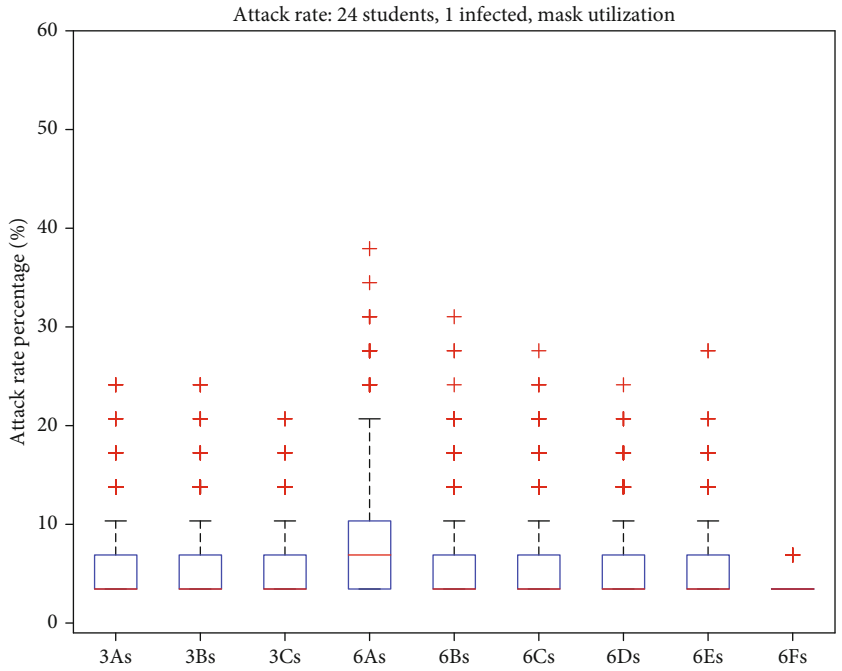

FIGURE 20: Boxplots indicating the 25th-75th percentile range representing the attack rate for those scenarios with 24 students and mask utilization and subject-0 being a student. As a comparison, the results of the same scenarios without mask utilization can be found in Figure 11, Section 3.2.

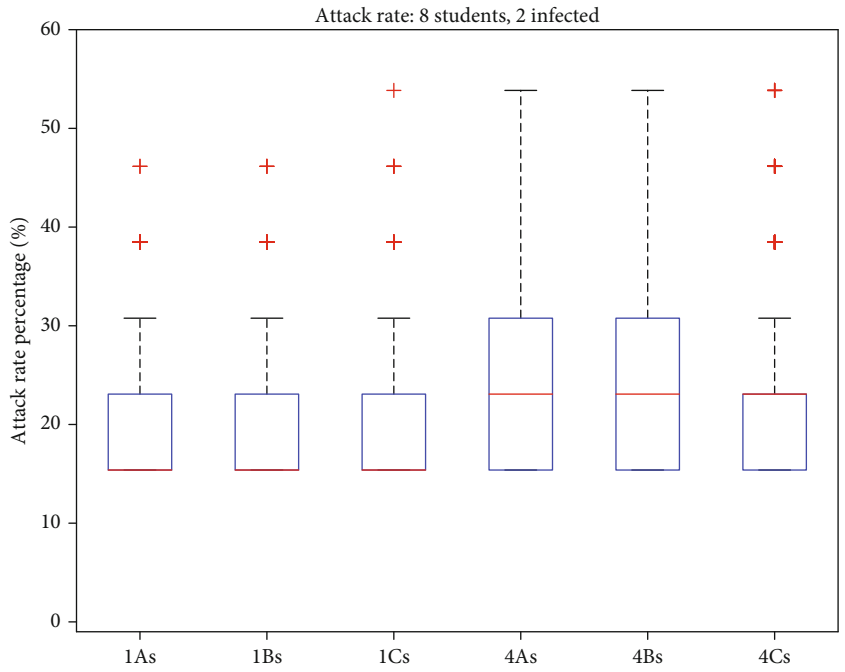

Figure 21: Boxplots indicating the 25th-75th percentile range representing the attack rate for those scenarios with 8 students and 2 subjects-0.

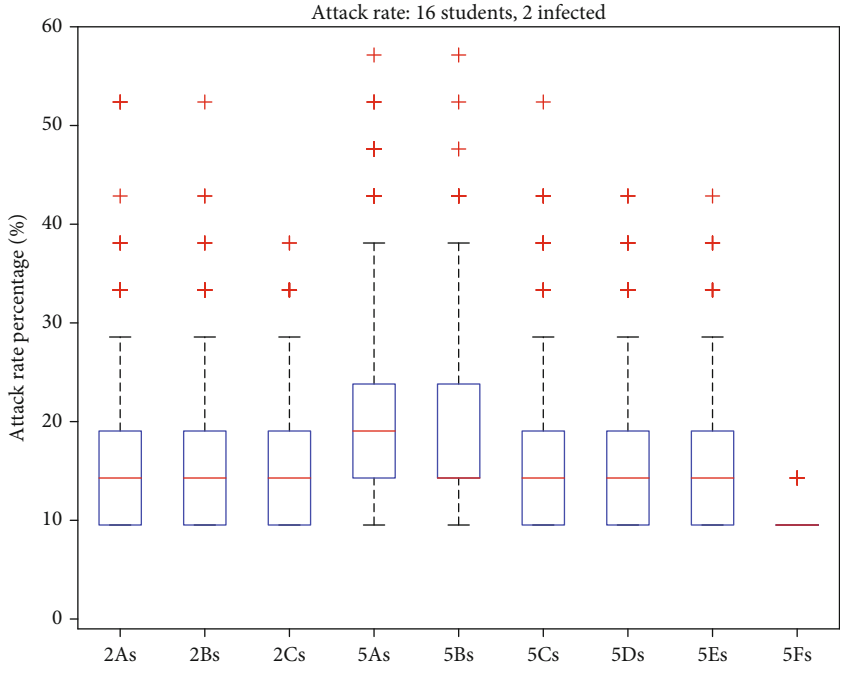

Figure 22: Boxplots indicating the 25th-75th percentile range representing the attack rate for those scenarios with 16 students and 2 subjects-0.

and more advanced solutions are needed. In fact, by looking at Figure 15, it can be noticed that even with the combined action of CO_2-based controls and the opening of windows, it is barely possible to keep the CO_2 concentrations around 1000 ppm. COVID-19 quanta concentration can be lowered almost to zero, but as soon as the windows are closed, it increases quickly.

Finally, by considering the cluster with 24 students (Figure 16), it is possible to observe that the combined action of CO_2 concentration-based mechanical ventilation and windows opening is incapable to obtain the same results found in the case of lower occupancy density if the door is closed. Consequently, all available means to provide additional fresh

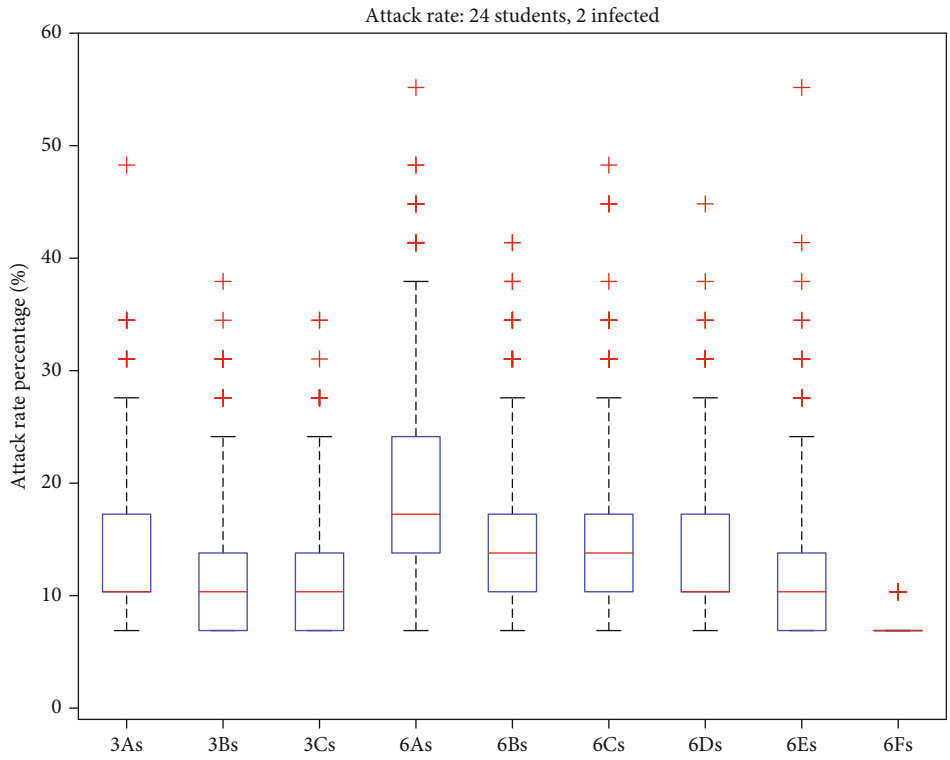

Figure 23: Boxplots indicating the 25th-75th percentile range representing the attack rate for those scenarios with 24 students and 2 subjects-0.

air, including natural ventilation solutions, should be always used to reduce the probability of infection.

As mentioned above, natural ventilation can be useful to further reduce the risk of contagion for those scenarios with a high number of susceptible subjects, where the combination of mechanical ventilation and the open door fails to keep the concentration level under an acceptable threshold. It is interesting to notice in the chart of the COVID-19 quanta concentrations (Figure 17) that opening the windows occasionally during the occupancy time (case 5Es) is more effective than opening them just every two hours and during the lunch break (case 5Ds). Considering the integral mean value of the quanta concentration, significantly lower values are calculated in case 5Es ($8.0E-4$ quanta m^{-3}) with respect to case 5Ds ($6.7E-4$ quanta m^{-3}). The quanta concentration is, as expected, negligible in case 5F, since the windows are left open during the whole occupancy time ($6.9E-6$ quanta m^{-3}).

3.2.4. Mask Utilization. Further analyses focused on measures were adopted to reduce the risk, such as the adoption of facial masks. Since it was established that higher attack rate values may be expected in those cases with a student as the initial infected subject when the occupancy density is high, only those scenarios with a student as subject-0 were evaluated again by taking into account also mask utilization. It was hypothesized that masks are used by all subjects all the time, and their effect was accounted for by reducing the probability of being infected by 33% [44]. The results are depicted below in Figures 18–20.

The results show that mask utilization can be useful to further reduce the risk of contagion, and in particular, it has the potential to reduce the probability of unacceptable outcomes especially in those scenarios with a crowded classroom. As expected, the effect of mask utilization is negligible when few students are present in the room. This result is expected since the way masks are accounted for is by reducing the individual probability of infection by a percentage value applied to the risk. For this reason, if the probability of infection is already low because of the low number of occupants in the classroom, mask utilization has a reduced effect on the attack rate.

3.2.5. Number of Initial Infected Subjects. Finally, other 24 scenarios have been run, by increasing the number of initially infected students from 1 to 2 (i.e., at day 0 in the classroom, two subjects-0, both students, are present simultaneously). The results are reported below in Figures 21–23 and show that the contagion risk rises significantly, especially if the occupancy density is high. In fact, in all scenarios, the median value is equal to or greater than 10%, with values close to 20% in some cases. In the case of low-density occupancy, a strong impact on the results is given by the door status: if it is closed, then it is possible to reach attack rate values of more than 50% (5 people infected), contrary to the case with only one subject-0 with a maximum of about 20%. In case two asymptomatic subjects are simultaneously present in the classroom at their symptoms' onset day, a combination of mechanical ventilation with CO_2-based controls and natural ventilation is always necessary to maintain the risk acceptable. By considering scenario 6As (Figure 23), where neither of these two ventilation strategies is employed, the 75th percentile of attack rate is about 40%, meaning that it is possible for more than 9 subjects to be infected before the school is closed or before all the subjects

become no longer contagious. The median value of the attack rate is about 20%, meaning that 5 infected subjects are expected before an ending condition.

4. Conclusions

In this work, the efficacy of three standard and dynamic ventilation strategies has been investigated, which are conventionally used for CO_2 concentration reduction, to mitigate the SARS-CoV-2 infection risk in a case study university classroom for 25 students (classroom E5.21 of Free University of Bozen-Bolzano, Italy). A Monte Carlo model has been developed to overcome the limitations of the state-of-the-art tools for COVID-19 risk assessment, related to the uncertainty of the boundary conditions, and coupled with building simulations to perform a dynamic assessment of the contagion risk.

A total of 96 scenarios have been evaluated, considering different ventilation strategies, door status, typology of subject-0, mask utilization, and the number of students in the classroom. For each scenario, 1000 Monte Carlo iterations have been run, counting the final number of infected subjects for each iteration and dividing it by the number of susceptible subjects, calculating in this way the attack rate. The Monte Carlo model has been coupled with a building model, to dynamically assess the dose received by the susceptible subjects, and with the airborne infection risk calculator (AIRC) tool, to evaluate the individual infection risk.

From the results, it is possible to conclude that

(i) For a classroom with 8–24 students, the outcome of an outbreak is independent of the subject-0 being a student or a professor if the latter is present for a limited amount of time (for these scenarios, about 20% of the students' occupancy time)

(ii) The door status (open or closed) has a significant effect on the attack rate, both on the average number of infected occupants and on the likelihood of an unacceptable outcome to happen

(iii) A strict correlation between ventilation strategies and occupancy density has been highlighted by the results. CO_2-based strategies are effective if the occupancy density is medium–high (16-24 students) but struggle to reduce the risk of infection if the density is low, since it is more difficult to reach the activation thresholds to activate the mechanical ventilation. For this reason, it is necessary to combine different solutions (e.g., mixed-mode ventilation and facial masks) to limit the risk for both students and lecturers. Furthermore, in case of high density, if it is not possible to keep the door open, it may be necessary to increase the ventilation rate by opening the windows as well to ensure an acceptable risk of infection

(iv) The number of elapsed days needed to complete the risk assessment for a scenario highlights the necessity of high ventilation rates as a prevention strategy. In fact, in some cases, an iteration requires more than two or three weeks before meeting an ending condition, usually involving a high number of infected asymptomatic subjects present in the classroom. These subjects increase the risk of contagion not only for other students and professors, with the potential to lead to unacceptable outcomes if more than one is present in the classroom at the same time, but also for other people outside the university

(v) Facial masks have the potential to reduce the probability of unacceptable outcomes, especially in those scenarios with high occupation density

(vi) If two subjects-0 are present simultaneously at day 0, then the combined action of mechanical ventilation with CO_2-based control and natural ventilation is always required to maintain the risk acceptable

Finally, some additional considerations can be made. It is important to limit the number of students that can be present in the classroom simultaneously, especially when only mechanical ventilation is available, and the door cannot be left open. Furthermore, even in a low-crowded classroom, mechanical ventilation may not be sufficient to keep COVID-19 quanta concentrations within acceptable levels if CO_2 concentration-based controls are adopted. For these cases, it is mandatory to keep the door open and/or to introduce natural ventilation, since the effect on infection probability reduction given by mask utilization is not as effective as for rooms with high occupancy density.

In those cases where the mechanical ventilation was not sized properly, then natural ventilation may be helpful, especially for a crowded classroom, when aided by an open door, to reduce the quanta dose received by the subjects to acceptable levels. In this case, the windows should be opened shortly and often during occupancy hours, rather than for a longer interval of time but only during break hours. Finally, mask utilization is helpful in terms of risk reduction since it has the effect to reduce the attack rate spread, lowering the probability of unacceptable outcomes, especially for crowded classrooms.

The presented methodology may be used also for more complex cases to compare different ventilation strategies especially if it is not feasible to adopt a deterministic approach for risk assessment. Furthermore, other distribution curves can be implemented to consider the emission rates related to different activities also in the case of COVID-19 variants, for example, the Delta and Omicron variants. Total and partial vaccinations may also be considered for different variants and for different percentages of vaccination coverage of the susceptible subjects. Finally, it is possible to extend the risk assessment also to multizone cases thanks to the coupling of the presented Monte Carlo model with building simulation software able to dynamically evaluate the airflows in a building.

Data Availability

The data regarding the simulations' results used to support the findings of this study are available from the corresponding author upon request.

Conflicts of Interest

The authors declare that they have no conflicts of interest.

Acknowledgments

This work was supported by the Open Access Publishing Fund of the Free University of Bozen-Bolzano.

References

[1] M. I. Mitova, C. Cluse, C. G. Goujon-Ginglinger, S. Kleinhans, M. Rotach, and M. Tharin, "Human chemical signature: investigation on the influence of human presence and selected activities on concentrations of airborne constituents," *Environmental Pollution*, vol. 257, article 113518, 2020.

[2] World Health Organization, *WHO Guidelines for Indoor Air Quality: Selected Pollutants*, World Health Organization, 2010.

[3] H. Tang, Y. Ding, and B. Singer, "Interactions and comprehensive effect of indoor environmental quality factors on occupant satisfaction," *Building and Environment*, vol. 167, article 106462, 2020.

[4] D. Lukcso, T. L. Guidotti, D. E. Franklin, and A. Burt, "Indoor environmental and air quality characteristics, building-related health symptoms, and worker productivity in a federal government building complex," *Archives of Environmental & Occupational Health*, vol. 71, no. 2, pp. 85–101, 2016.

[5] D. P. Wyon, "The effects of indoor air quality on performance and productivity," *Indoor Air*, vol. 14, Supplement 7101 pages, 2004.

[6] M. Frontczak and P. Wargocki, "Literature survey on how different factors influence human comfort in indoor environments," *Building and Environment*, vol. 46, no. 4, pp. 922–937, 2011.

[7] M. J. Mendell, E. A. Eliseeva, M. Spears et al., "A longitudinal study of ventilation rates in California office buildings and self-reported occupant outcomes including respiratory illness absence," *Building and Environment*, vol. 92, pp. 292–304, 2015.

[8] D. K. Milton, P. M. Glencross, and M. D. Walters, "Risk of sick leave associated with outdoor air supply rate, humidification, and occupant complaints," *Indoor Air*, vol. 10, no. 4, 2000.

[9] T. A. Myatt, J. Staudenmayer, K. Adams, M. Walters, S. N. Rudnick, and D. K. Milton, "A study of indoor carbon dioxide levels and sick leave among office workers," *Environmental Health: a Global Access Science Source*, vol. 1, no. 1, p. 3, 2002.

[10] M. Lahtinen, C. Sundman-Digert, and K. Reijula, "Psychosocial work environment and indoor air problems: a questionnaire as a means of problem diagnosis," *Occupational and Environmental Medicine*, vol. 61, no. 2, pp. 143–149, 2004.

[11] Z. Bako-Biro, "Human perception, SBS sympsoms and performance of office work during exposure to air polluted by building materials and personal computers," *International Centre for Indoor Environment and Energy*, vol. 2, 2004.

[12] R. Maddalena, M. J. Mendell, K. Eliseeva et al., "Effects of ventilation rate per person and per floor area on perceived air quality, sick building syndrome symptoms, and decision-making," *Indoor Air*, vol. 25, no. 4, 2015.

[13] P. Wargocki, J. Sundell, W. Bischof et al., "Ventilation and health in non-industrial indoor environments: report from a European multidisciplinary scientific consensus meeting (EUROVEN)," *Indoor Air*, vol. 12, no. 2, 2002.

[14] American Society of Heating Refrigerating and Air-Conditioning Engineers, *ANSI/ASHRAE standard 62.1-2022 ventilation for acceptable indoor air quality*, American Society of Heating, Refrigerating and Air-Conditioning Engineers, 2022.

[15] American Society of Heating Refrigerating and Air-Conditioning Engineers, *ANSI/ASHRAE Standard 62.2-2022 "Ventilation and Acceptable Indoor Air Quality in Low-Rise Residential Buildings"*, American Society of Heating, Refrigerating and Air-Conditioning Engineers, 2022.

[16] S. Sadrizadeh, R. Yao, F. Yuan et al., "Indoor air quality and health in schools: a critical review for developing the roadmap for the future school environment," *Journal of Building Engineering*, vol. 57, article 104908, 2022.

[17] P. Kumar, A. B. Singh, T. Arora, S. Singh, and R. Singh, "Critical review on emerging health effects associated with the indoor air quality and its sustainable management," *Science of the Total Environment*, vol. 872, p. 162163, 2023.

[18] L. R. López, P. Dessì, A. Cabrera-Codony et al., "CO_2 in indoor environments: from environmental and health risk to potential renewable carbon source," *Science of The Total Environment*, vol. 856, article 159088, 2023.

[19] N. Muscatiello, A. McCarthy, C. Kielb, W. H. Hsu, S. A. Hwang, and S. Lin, "Classroom conditions and CO_2 concentrations and teacher health symptom reporting in 10 New York state schools," *Indoor Air*, vol. 25, no. 2, 2015.

[20] I. Annesi-Maesano, N. Baiz, S. Banerjee, P. Rudnai, S. Rive, and the SINPHONIE Group, "Indoor air quality and sources in schools and related health effects," *Journal of Toxicology and Environmental Health, Part B, Critical Reviews*, vol. 16, no. 8, pp. 491–550, 2013.

[21] D. G. Shendell, R. Prill, W. J. Fisk, M. G. Apte, D. Blake, and D. Faulkner, "Associations between classroom CO_2 concentrations and student attendance in Washington and Idaho," *Indoor Air*, vol. 14, no. 5, 2004.

[22] G. Smedje and D. Norbäck, "New ventilation systems at select schools in Sweden–effects on asthma and exposure," *Archives of Environmental Health*, vol. 55, no. 1, pp. 18–25, 2000.

[23] Z. Bakó-Biró, D. J. Clements-Croome, N. Kochhar, H. B. Awbi, and M. J. Williams, "Ventilation rates in schools and pupils' performance," *Building and Environment*, vol. 48, no. 1, pp. 215–223, 2012.

[24] J. Toftum, B. U. Kjeldsen, P. Wargocki, H. R. Menå, E. M. N. Hansen, and G. Clausen, "Association between classroom ventilation mode and learning outcome in Danish schools," *Building and Environment*, vol. 92, pp. 494–503, 2015.

[25] L. Chatzidiakou, D. Mumovic, and A. J. Summerfield, "What do we know about indoor air quality in school classrooms? A critical review of the literature," *Intelligent Buildings International*, vol. 4, no. 4, pp. 228–259, 2012.

[26] L. Stabile, M. Dell'Isola, A. Russi, A. Massimo, and G. Buonanno, "The effect of natural ventilation strategy on indoor air quality in schools," *The Science of the Total Environment*, vol. 595, pp. 894–902, 2017.

[27] R. Almeida, M. Pinto, P. Pinho, and L. Lemos, "Natural ventilation and indoor air quality in educational buildings: experimental assessment and improvement strategies," *Energy Efficiency*, vol. 10, no. 4, pp. 839–854, 2017.

[28] L. Stabile, A. Massimo, L. Canale, A. Russi, A. Andrade, and M. Dell'Isola, "The effect of ventilation strategies on indoor air quality and energy consumptions in classrooms," *Buildings*, vol. 9, no. 5, p. 110, 2019.

[29] S. Burgmann and U. Janoske, "Transmission and reduction of aerosols in classrooms using air purifier systems," *Physics of fluids*, vol. 33, no. 3, article 033321, 2021.

[30] G. Buonanno, L. Morawska, and L. Stabile, "Quantitative assessment of the risk of airborne transmission of SARS-CoV-2 infection: prospective and retrospective applications," *Environment International*, vol. 145, article 106112, 2020.

[31] A. Di Gilio, J. Palmisani, M. Pulimeno et al., "CO_2 concentration monitoring inside educational buildings as a strategic tool to reduce the risk of Sars-CoV-2 airborne transmission," *Environmental Research*, vol. 202, article 111560, 2021.

[32] S. Park, Y. Choi, D. Song, and E. K. Kim, "Natural ventilation strategy and related issues to prevent coronavirus disease 2019 (COVID-19) airborne transmission in a school building," *The Science of the Total Environment*, vol. 789, article 147764, 2021.

[33] E. C. Riley, G. Murphy, and R. L. Riley, "Airborne spread of measles in a suburban elementary school," *American Journal of Epidemiology*, vol. 107, no. 5, pp. 421–432, 1978.

[34] G. Buonanno, L. Stabile, and L. Morawska, "Estimation of airborne viral emission: quanta emission rate of SARS-CoV-2 for infection risk assessment," *Environment International*, vol. 141, article 105794, 2020.

[35] G. Pernigotto and A. Gasparella, *Conference proceedings of Roomvent 2020*, Centro Congressi Internazionale srl, Turin, Italy, 2021.

[36] President of the Italian Republic, "Decree of the President of the Italian Republic (DPR) n. 412 of the 26th August 1993, "Regolamento recante norme per la progettazione, l'installazione, l'esercizio e la manutenzione degli impianti termici degli edifici ai fini del contenimento dei consumi di energia," Italian Government, 1993.

[37] H.-C. Hsu, C.-Y. Pan, I.-C. Wu, C.-C. Liu, and Z.-Y. Zhuang, "Using the big data analysis and basic information from lecture halls to predict air change rate," *Journal of Building Engineering*, vol. 66, pp. 105817–107102, 2023.

[38] American Society of Heating Refrigerating and Air-Conditioning Engineers, *2021 ASHRAE Handbook: Fundamentals (SI)*, American Society of Heating, Refrigeration and Air-Conditioning Engineers, 2021.

[39] A. Persily and L. de Jonge, "Carbon dioxide generation rates for building occupants," *Indoor Air*, vol. 27, no. 5, 2017.

[40] P. Penna, F. Cappelletti, F. Tahmasebi, and A. Mahdavi, "Multi-stage calibration of the simulation model of a school building through short-term monitoring," *Electronic Journal of Information Technology in Construction*, vol. 20, pp. 132–145, 2015.

[41] CEN, "EN 16798-1:2019- Energy Performance of Buildings - Ventilation for Buildings - Part 1: Indoor Environmental Input Parameters for Design and Assessment of Energy Performance of Buildings Addressing Indoor Air Quality, Thermal Environment, Lighting and Acoustics - Module M1-6," European Committee for Standardization, 2019.

[42] L. Gammaitoni and M. C. Nucci, "Using a mathematical model to evaluate the efficacy of TB control measures," *Emerging Infectious Diseases*, vol. 3, no. 3, pp. 335–342, 1997.

[43] K. A. Walsh, S. Spillane, L. Comber et al., "The duration of infectiousness of individuals infected with SARS-CoV-2," *The Journal of Infection*, vol. 81, no. 6, pp. 847–856, 2020.

[44] A. Mikszewski, G. Buonanno, L. Stabile, A. Pacitto, and L. Morawska, *Airborne Infection Risk Calculator (AIRC) User's Manual, v. 3.0 Beta*, 2021.

[45] S. A. Lauer, K. H. Grantz, Q. Bi et al., "The incubation period of coronavirus disease 2019 (COVID-19) from publicly reported confirmed cases: estimation and application," *Annals of Internal Medicine*, vol. 172, no. 9, pp. 577–582, 2020.

[46] X. He, E. Lau, P. Wu et al., "Temporal dynamics in viral shedding and transmissibility of COVID-19," *Nature Medicine*, vol. 26, no. 5, pp. 672–675, 2020.

[47] Q. Ma, J. Liu, Q. Liu et al., "Global percentage of asymptomatic SARS-CoV-2 infections among the tested population and individuals with confirmed COVID-19 diagnosis: a systematic review and meta-analysis," *JAMA Network Open*, vol. 4, no. 12, article e2137257, 2021.